Synthesis of Symmetric and Dissymmetric Star-shaped Pentaarylcyclopentadienyl Ru(II) Complexes Containing Styryl-BODIPY Fragments

Melissa Dumartin,[1] Seifallah Abid,[1] Yohan Gisbert,[1] Nathalie Saffon-Merceron,[2] Sheng Gao,[3] Nicola Armaroli,[3] Barbara Ventura,[3] Claire Kammerer,*[1] Gwénaël Rapenne*[1,4]

[1]*CEMES, Université de Toulouse, CNRS, 29 rue Marvig, F-31055 Toulouse Cedex 4, France*

[2]*Université de Toulouse, UPS, ICT UAR2599, 118 route de Narbonne, F-31062 Toulouse, France*

[3]*Istituto per la Sintesi Organica e la Fotoreattività, CNR-ISOF, Via Gobetti 101, 40129 Bologna, Italy*

[4]*Division of Materials Science, Nara Institute of Science and Technology, NAIST, 8916-5 Takayama-cho, Ikoma, Nara 630-0192, Japan*

E-mail: rapenne@cemes.fr

We synthesised star-shaped ruthenium(II) complexes containing one or five styryl-BODIPY units arranged around a central trisindazolylrutheniumcyclopentadienyl fragment. A symmetric complexe was obtained following a five-fold Suzuki-Miyaura reaction of the pentabrominated key precursor while desymmetrisation was next achieved *via* a modular synthetic approach based on sequential chemoselective Suzuki-Miyaura reactions on a key building block bearing one iodophenyl and four bromophenyl groups.

Keywords: Ruthenium, BODIPY, Desymmetrization

With the ultimate goal to create complex nanomachineries,[1] various types of molecular motors[2] or gears[3] have been designed but only a few are based on coordination complexes. With a large number of metals and a wide variety of ligands available, coordination chemistry is a very versatile and efficient tool to assemble mechanical subunits to prepare synthetic molecular machines.[4] In the last decade, we designed and synthesised a series of star-shaped molecular motors[5] and gears subunits[6] based on heteroleptic ruthenium(II) complexes containing a hydrotris(indazolyl)-borate ligand as anchoring platform and a functionalised pentaarylcyclopentadienyl ligand as rotating subunit. These compounds interestingly exhibited controlled clockwise or anticlockwise unidirectional rotation once anchored on metallic surfaces.[7]

As nanosized movable entities, molecular machines can be fuelled by various sources of energy such as light, chemicals or electrons. Chemical fuels generate waste while addressing electrons at the single-molecule level remains highly challenging, so light appears to be a particularly clean and easy to operate as well as highly efficient and non-invasive source of energy.[8] In our efforts to expand the set of mechanical tasks performed by our rotary molecular machines, it was envisioned to exploit light as a stimulus and integrate a photoactivable function in their design, allowing for instance the light-induced engagement or disengagement of cogwheels within a train of molecular gears. It is thus of prime importance to explore the possibility to incorporate various kinds and numbers of photoactive subunits in the backbone of our ruthenium(II)-based molecular motors and gears. This goal requires the development of synthetic strategies allowing to obtain not only symmetric structures but also desymmetrised complexes, which are more challenging to be prepared but also more promising in terms of properties as shown for obtaining high unidirectionality in previously reported molecular motors.[7]

In our effort to build up such photoactive systems, we report in this paper the synthesis of extended star-shaped molecules based on pentaarylcyclopentadienyl ruthenium(II) complexes functionalised with five peripheral photoactive BODIPY units. In a preliminary work, the photophysical properties of such complexes were investigated, demonstrating that they are viable platforms for the creation of systems that can be photoactivated.[9] To this end, two strongly fluorescent BODIPYs were selected: **B1** as a standard fluorescent BODIPY fragment and **B2** as a derivative incorporating two photochemically isomerisable styryl groups on the pyrrole α-positions for photo-mechanical applications. The symmetric ruthenium(II) complex **B2$_5$[Ru]** was then synthesised as well as a desymmetrised ruthenium(II) complex with four BODIPYs and one styryl-BODIPY **B1$_4$B2$_1$[Ru]** (Scheme 1 and 2). The parent compound **B1$_5$[Ru]** has been previously synthesised[10] but the absence of photochemically isomerisable styryl groups drastically limits its potentialities in light-induced motions.

Our general strategy for the synthesis of the symmetric target compound **B2$_5$[Ru]** relies on the post-functionalisation of a ruthenium(II) complex as key intermediate, incorporating a thioether-functionalised hydrotris(indazolyl)borate tripod in combination with a penta(*p*-halogenophenyl)cyclopentadienyl ligand.[11] A variety of transition metal-catalysed cross-coupling reactions are tolerated, which leads in a divergent manner to a family of piano-stool ruthenium complexes with a five-fold substituted cyclopentadienyl ligand, exhibiting potential mechanical functions stimulated by light. However, when desymmetrised cyclopentadienyl units are desired, the synthetic strategy appeared to be much more chalenging than anticipated. In the course of our previous work towards desymmetrised complexes, we explored the chemoselective functionalization of penta(4-halogenophenyl)cyclopenta-dienyl ruthenium complex **Br$_4$I$_1$[Ru]** incorporating a single aryl iodide moiety. The discrimination of aryl iodides over bromides, although largely exploited in cross-couplings such as Sonogashira or Stille couplings, remains difficult in the case of Suzuki-Miyaura coupling, due to a change of rate-determining step in the catalytic cycle. In a previous paper,[6c] we reported the successful single Suzuki-Miyaura cross-coupling of complex **Br$_4$I$_1$[Ru]** using copper(I) thiophene-2-carboxylate (CuTC) as a stoichiometric additive in the presence of the mild $Pd(PPh_3)_4$ catalyst in THF. Unfortunately, these conditions are restricted to the use of boronic acids as coupling partners, since an

interaction between the latter and CuTC is expected to occur prior to the actual coupling. Indeed, when these conditions were tested for the coupling of precursor **Br_4I_1[Ru]** with boronic ester **B2**, no conversion was observed. Since boronic acid function should be avoided in **B2** due to the presence of amino groups, we explored alternative reaction conditions that could favour a chemoselective functionalization of **Br_4I_1[Ru]** in the presence of a boronic ester.

The styryl-BODIPY **B2** was prepared from BODIPY **B1** *via* a double Knœvenagel condensation with *p*-dimethylaminobenzaldehyde in the presence of piperidine and acetic acid. The reaction was run in refluxing toluene and a Dean-Stark apparatus was used to trap water. The selective formation of *trans*-styryl moieties on both pyrrole α-positions was achieved with a 20% yield. This moderate yield is mostly related to purification issues. **B2** was characterised by mass spectrometry as well as ^{1}H, ^{13}C, ^{11}B and ^{19}F NMR spectroscopy. The ^{19}F NMR spectrum of **B2** exhibits a quadruplet shifted to -139.1 ppm with a coupling constant *J* (^{11}B-^{19}F) of 35.0 Hz. The *trans*-configuration of the *p*-dimethylaminostyryl fragments was unambiguously confirmed by ^{1}H NMR spectroscopy, which revealed a 16.6 Hz coupling constant between vinylic protons. Next, styryl-BODIPY derivative **B2** was used as coupling partner in a Suzuki-Miyaura reaction with key intermediate **Br_5[Ru]** in the presence of $Pd(OAc)_2$/SPhos as catalytic system and K_3PO_4 as base, to afford the five-fold substituted target compound **$B2_5$[Ru]** in 74% yield (Scheme 1), corresponding to 94% yield per newly-formed C-C bond. The use of a biphasic solvent system combining toluene/ethanol/water (2:2:1) is the key to increase the reaction efficiency. Without this biphasic solvent system, only trace amounts of **$B2_5$[Ru]** were observed. **$B2_5$[Ru]** was characterised by mass spectrometry as well as ^{1}H, ^{13}C, ^{11}B and ^{19}F NMR spectroscopy. In the ^{1}H NMR spectrum (Fig. S5), integration of the two AA'BB' systems corresponding to the 4,4'-biphenyl linkers and of the methyl and ethyl groups located on the pyrrole rings, as compared to protons belonging to the equivalent indazole rings shows that five styryl-BODIPY moieties have been grafted. In addition, the coupling constant of 16.4 Hz between the two sets of 10 vinyl protons confirms the *trans*-geometry of the styryl units. Finally, both the ^{11}B and ^{19}F NMR spectra (Fig. S7 and Fig. S8) exhibit a single signal located at 1.32 ppm and -139.1 ppm, respectively, in agreement with the chemical shifts observed for the BODIPY unit of precursor **B2**. This indicates that all styryl-BODIPYs are equivalent in this five-fold substituted ruthenium complex.

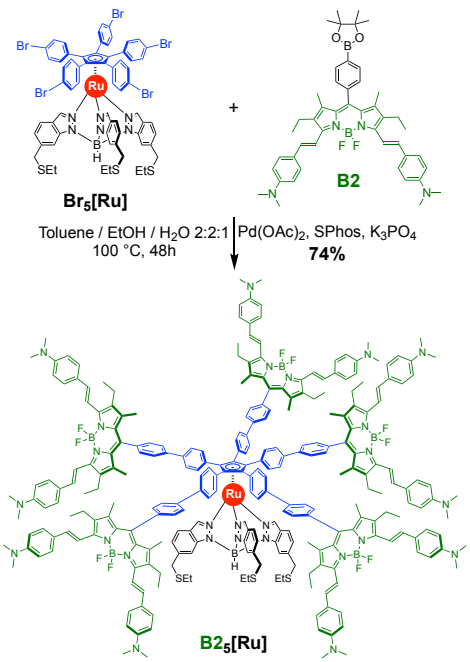

Scheme 1. Synthesis of the symmetric **$B2_5$[Ru]** starting from **Br_5[Ru]**.

To synthesise the desymmetrised complex **$B1_4B2_1$[Ru]** bearing different BODIPYs, the penta(*p*-halogenophenyl)cyclopentadienyl ruthenium(II) key building block, incorporating a single *p*-iodophenyl group (**Br_4I_1[Ru]**, Scheme 2) was prepared.[6] Thanks to the difference in reactivities of aryl iodides *vs* bromides in palladium-catalysed cross-couplings, this platform was expected to allow the sequential introduction of substituents on the cyclopentadienyl ligand to yield desymmetrised ruthenium complexes in a controlled manner.

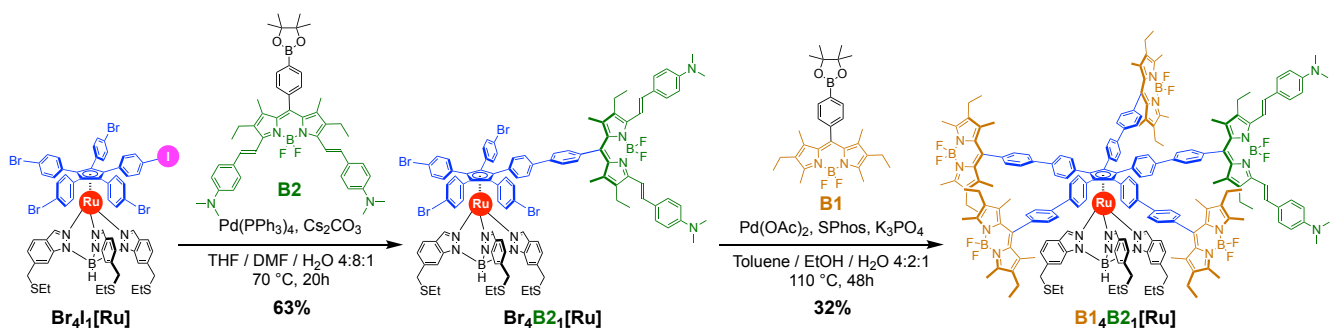

Scheme 2. Synthesis of the desymmetrised star-shaped Ru-based system **$B1_4B2_1$[Ru]** starting from key intermediate **Br_4I_1[Ru]**.

As already explained, boronic acid function should be avoided in **B2** due to the presence of amino groups. Then, we explored alternative reaction conditions that could favour a chemoselective functionalization of **Br_4I_1[Ru]** in the presence of a boronic ester. We already knew that the conditions used for the coupling of **Br_5[Ru]** with **B1** or **B2** (*i.e.* $Pd(OAc)_2$, SPhos, K_3PO_4 in toluene/EtOH/H_2O at 100 °C) lead to very efficient coupling of aryl bromides and would thus be detrimental to a chemoselective coupling. We thus turned to conditions used previously in our group for the statistical monocoupling of **Br_5[Ru]** (*i.e.* $PdCl_2(dppf)$, Cs_2CO_3 in DMF/H_2O at 100 °C),[12] employing a less activated catalyst such as $Pd(PPh_3)_4$ and lowering the temperature to 70 °C to favour the oxidative addition of the weaker C-I bond (Scheme 2).[6] This strategy proved to be successful, and the coupling of **Br_4I_1[Ru]** with **B2** took place with high chemoselectivity to give rise to **Br_4B2_1[Ru]** in 63% yield via a single Suzuki-Miyaura coupling. The four remaining *p*-bromophenylene groups were subsequently submitted to distinct Suzuki-Miyaura coupling conditions in the presence of an excess of BODIPY-derivative **B1**. Compared with the conditions for iodophenylene functionalisation, the $Pd(OAc)_2$/SPhos catalytic system was employed here in combination with K_3PO_4 as base at a higher temperature (110 °C). Again, the use of a biphasic solvent system combining toluene/ethanol/water (4:2:1) appeared crucial. The desymmetrised target complex **$B1_4B2_1$[Ru]** was obtained in 32% yield, thus corresponding to 75% yield per single C-C coupling.

Both complexes were characterised by mass spectrometry as well as ^{1}H, ^{13}C, ^{11}B and ^{19}F NMR spectroscopy. Looking in detail at the ^{1}H-NMR in the 7.9-8.2 ppm region, two signals corresponding to the indazol ring (Fig S13, protons a and b) are surrounded by small signals integrating for a few %. Since the MALDI-TOF MS spectrum showed one single peak, we believe this signals correspond to isomers with the alkene bond of the **B2** fragment in the Z configuration. Due to the loss of C_s symmetry on the cyclopentadienyl ligand, the ^{1}H and ^{13}C NMR spectra are more complex (Fig. S13 and Fig. S14, respectively, for **$B1_4B2_1$[Ru]**) compared to the BODIPY-substituted symmetric counterpart **$B2_5$[Ru]**. In the ^{1}H NMR spectrum of intermediate **Br_4B2_1[Ru]** (Fig. S9), integration of the methyl and ethyl groups located on the pyrrole rings, as compared to protons belonging to the equivalent indazole rings, clearly shows that a single styryl-BODIPY moiety has been coupled. The *trans*-configuration of the styryl groups is again confirmed by the 17.0 Hz coupling constant between the vinyl protons. In the case of the target complex **$B1_4B2_1$[Ru]**, the ^{19}F NMR spectrum (Figure 2) exhibits two distinct signals located at -139.3 ppm and -145.7 ppm, respectively, with an integral ratio of 1 to 4. These chemical shifts are in full agreement with those observed for precursors **B2** (-139.1 ppm) and **B1** (-145.7 ppm), which shows that the ruthenium(II) complex incorporates a single styryl-BODIPY unit combined with four BODIPY moieties. This is also confirmed by the integral ratios in the ^{1}H NMR spectrum and by mass spectrometry.

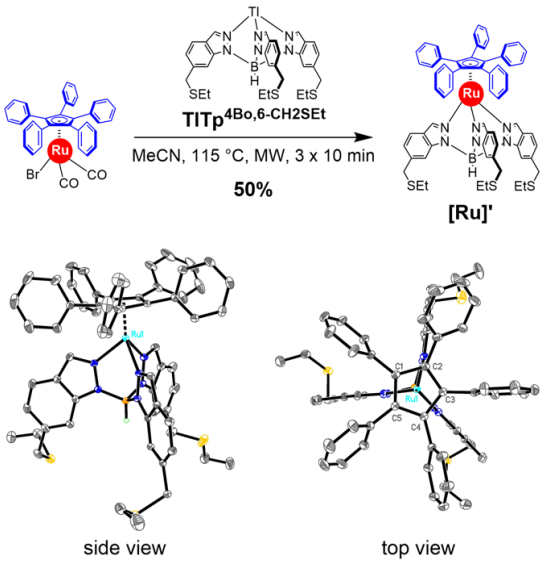

The model system **[Ru]'** incorporating a bare pentaphenylcyclopentadienyl ligand in combination with the thioether-functionalised hydrotris(indazolyl)borate tripod (Scheme 3), has been also synthesized to help in the assignment of the signals of ^{1}H and ^{13}C NMR spectra and to have an X-ray structure of the central part of our molecules.

Scheme 3. Synthesis of model compound **[Ru]'** (top), and side view (bottom left) and top view (bottom right) of the molecular structure of ruthenium complex **[Ru]'**. Thermal ellipsoids are drawn at 30% probability. Hydrogen atoms (except for B–H), solvent molecule and disordered atoms are omitted for clarity. The centroid of the cyclopentadienyl ligand is distant from the ruthenium atom by 1.80 Å and the average distance between the three coordinated nitrogens and the ruthenium centre is 2.14 Å.

This compound was synthesised starting from the known bromido dicarbonyl η^5-1,2,3,4,5-pentaphenylcyclopentadienyl ruthenium(II)[12] *via* a ligand exchange process in the presence of thallium hydrotris(indazolyl)borate **$TlTp^{4Bo,6\text{-}CH2SEt}$** [11] in acetonitrile under microwave irradiation (Scheme 3, top). Complex **[Ru]'** was obtained in 50% yield and fully characterised by mass spectrometry, elemental analysis and NMR spectroscopy. Single crystals were also obtained by slow evaporation of a 1:2 methanol/CH_2Cl_2 solution of complex **[Ru]'**, thus allowing the resolution of its structure by X-ray diffraction (Scheme 3, bottom). The X-ray structure is similar to previous structures obtained for this family of Ru(II) complexes[5,6] bearing a pentaphenylcyclopentadienyl and a trisindazolylborate ligand with the later binding in a facial tripodal mode (i.e. κ^3-*N*,*N*',*N*''). The complex has a piano stool structure with the cp ligand fitting in the vacant spaces of the tripodal ligand.

The absorption spectra of **B1**, **B2**, **$B2_5$[Ru]** and **$B1_4B2_1$[Ru]** were recorded in CH_2Cl_2 at 298 K (Figure 4). The main absorption parameters are collected for each compound in the experimental section. Complexes **$B2_5$[Ru]** and **$B1_4B2_1$[Ru]** show an intense band in the UV region peaked around 270 nm like analogous ruthenium

complexes[9] with similar molar absorption coefficients. In the visible region, the absorption spectra of **B2** and **B2$_5$[Ru]** are similar, with an absorption peak around 710 nm. Compared with **B1** which exhibit an absorption peak around 525 nm, and due to the effect of styryl fragments, the absorption spectra of **B2** and **B2$_5$[Ru]** are red-shifted. As expected, the extinction coefficient of **B2$_5$[Ru]** is almost five times higher than that of **B2**, in line with the presence of five styryl-BODIPY moieties in the complex. Finally, **B1$_4$B2$_1$[Ru]**, with four BODIPY and one styryl-BODIPY arms, exhibits both the absorption features at 526 nm (from **B1**) and 711 nm (from **B2**) with an intensity about four times larger than that of **B1** and almost equal to **B2** at their respective absorption wavelengths. This illustrates the additivity of the absorption features of the different chromophores in this compound.

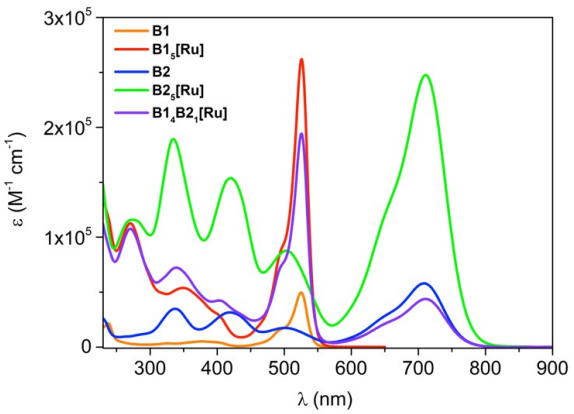

Figure 1. Absorption spectra of compounds **B1**, **B1$_5$[Ru]**, **B2**, **B2$_5$[Ru]** and **B1$_4$B2$_1$[Ru]** in CH_2Cl_2 at 298 K.

In conclusion, star-shaped ruthenium(II) complexes incorporating one (**B1$_4$B2$_1$[Ru]**), or five (**B2$_5$[Ru]**) photoisomerisable styryl-BODIPY units (**B2**) have been synthesised and characterised by ^{1}H, ^{13}C, ^{11}B and ^{19}F NMR spectroscopy, absorption and HR-mass spectrometry. The symmetric complex **B2$_5$[Ru]** was obtained following a five-fold Suzuki-Miyaura coupling with the corresponding BODIPY-substituted phenylboronic acid pinacol ester precursor **B2**. The dissymmetric **B1$_4$B2$_1$[Ru]** was obtained *via* two consecutive Suzuki-Miyaura chemoselective couplings under different conditions, starting from the preactivated key building block **Br$_4$I$_1$[Ru]**. The absorption spectra showed the additivity of the features of the different chromophores in the ruthenium(II) complexes containing five BODIPYs (**B1**), five styryl-BODIPYs (**B2**) and in the desymmetrised complex bearing four **B1** and one **B2** fragment. Work is now underway to investigate the photochemical and photophysical properties of these extended ruthenium complexes in more details, such as photoinduced electron and/or energy transfer processes. The *trans-cis* photoisomerisation of the styryl subunits will also be studied, with the goal to explore the potential of such ruthenium(II) complexes as mechanically-active components of photodeformable materials.

This work has received funding from the JSPS KAKENHI Grant-in-Aid for Challenging Research (20K21131), the JSPS KAKENHI Grant-in-Aid for Basic Research A (22H00325), the CNR (Project PHEEL) and the European Union's Horizon 2020 research and innovation program under the project MEMO (grant agreement No 766864). YG thanks the University Toulouse III Paul Sabatier for a PhD Fellowship. Special thanks are given to Ms. Yoshiko Nishikawa (NAIST) for her admirable contribution to the measurements of high mass compounds (MALDI).

References and Notes

1 V. Balzani, A. Credi and M. Venturi, *Molecular Devices and Machines. Concepts and Perspectives for the Nanoworld*, 2nd ed. Wiley-VCH, Weinheim, **2008**.

2 T. R. Kelly, H. De Silva and R. A. Silva, *Nature* **1999**, **401**, 150; N. Koumura, R. W. J. Zijlstra, R. A. van Delden, N. Harada, B. L. Feringa, *Nature* **1999**, *401*, 152; D. A. Leigh, J. K. Y. Wong, F. Dehez, F. Zerbetto, *Nature* **2003**, *424*, 174; M. von Delius, E. M. Geertsema, D. A. Leigh, *Nat. Chem.* **2010**, *2*, 96; H.-P. Jacquot de Rouville, R. Garbage, F. Ample, A. Nickel, J. Meyer, F. Moresco, C. Joachim and G. Rapenne, *Chem. Eur. J.*, 2012, **18**, 8925–8928; L. Greb, A. Eichhöfer, J.-M. Lehn, *Angew. Chem. Int. Ed.* **2015**, *54*, 14345; M. Guentner, M. Schildhauer, S. Thumser, P. Mayer, D. Stephenson, P. J. Mayer, H. Dube, *Nat. Commun.* **2015**, *6*, 8406; J. T. Foy, Q. Li, A. Goujon, J.-R. Colard-Itté, G. Fuks, E. Moulin, O. Schiffmann, D. Dattler, D. P. Funeriu, N. Giuseppone, *Nat. Nanotechnol.* **2017**, *12*, 540; S. Kassem, T. van Leeuwen, A. S. Lubbe, M. R. Wilson, B. L. Feringa, D. A. Leigh, *Chem. Soc. Rev.* **2017**, *46*, 2592; M. Baroncini, S. Silvi, A. Credi, *Chem. Rev.* **2020**, *120*, 200; D. Dattler, G. Fuks, J. Heiser, E. Moulin, A. Perrot, X. Yao, N. Giuseppone, *Chem. Rev.* **2020**, *120*, 310; V. García-López, D. Liu, J. M. Tour, *Chem. Rev.* **2020**, *120*, 79.

3 H. Ube, Y. Yasuda, H. Sato, M. Shionoya, *Nat. Commun.* **2017**, *8*, 14296; D. K. Frantz, A. Linden, K. K. Baldridge, J. S. Siegel, *J. Am. Chem. Soc.* **2012**, *134*, 1528; K. H. Au Yeung, T. Kühne, F. Eisenhut, M. Kleinwächter, Y. Gisbert, R. Robles, N. Lorente, G. Cuniberti, C. Joachim, G. Rapenne, C. Kammerer, F. Moresco, *J. Phys. Chem. Lett.* **2020**, *11*, 6892; Y. Gisbert, S. Abid, C. Kammerer, G. Rapenne, *Chem. Eur. J.* **2021**, *27*, 12019; A. Gerwien, F. Gnannt, P. Mayer, H. Dube, *Nat. Chem*. **2022**, *14*, 670.

4 A. Goswami, S. Saha, P. K. Biswas, M. Schmittel, *Chem. Rev.* **2020**, *120*, 125.

5 G. Vives, H.-P. Jacquot de Rouville, A. Carella, J.-P. Launay, G. Rapenne, *Chem. Soc. Rev.* **2009**, *38*, 1551; C. Kammerer, G. Rapenne, *Eur. J. Inorg. Chem*. **2016**, 2214.

6 Y. Gisbert, S. Abid, G. Bertrand, N. Saffon-Merceron, C. Kammerer, G. Rapenne, *Chem. Commun.* **2019**, *55*, 14689; Y. Gisbert, C. Kammerer, G. Rapenne, *Chem. Eur. J.,* **2021**, *27*, 16242; S. Abid, Y. Gisbert, M. Kojima, N. Saffon-Merceron, J. Cuny, C. Kammerer, G. Rapenne, *Chem. Sci*. **2021**, *12*, 4709; K. Omoto, M. Shi, K. Yasuhara, C. Kammerer and G. Rapenne, *Chem. Eur. J.*, **2023**, *29*, e202203483.

7 U. G. E. Perera, F. Ample, H. Kersell, Y. Zhang, G. Vives, J. Echeverria, M. Grisolia, G. Rapenne, C. Joachim, S.-W. Hla, *Nat. Nanotechnol.* **2013**, *8*, 46; Y. Zhang, J. P. Calupitan, T. Rojas, R. Tumbleson, G. Erbland, C. Kammerer, T. M. Ajayi, S. Wang, L.

A. Curtiss, A. T. Ngo, S. E. Ulloa, G. Rapenne, S.-W. Hla, *Nat. Commun.* **2019**, *10*, 3742.

8 V. Balzani, A. Credi, M. Venturi, *Chem. Soc. Rev.,* **2009**, *38*, 1542; S. Silvi, M. Venturi, A. Credi, *Chem. Commun.* **2011**, *47*, 2483.

9 S. Gao, Y. Gisbert, G. Erbland, S. Abid, C. Kammerer, A. Venturini, G. Rapenne, B. Ventura, N. Armaroli, *Phys. Chem. Chem. Phys.,* **2021**, *23*, 17049.

10 G. Erbland, S. Abid, Y. Gisbert, N. Saffon-Merceron, Y. Hashimoto, L. Andreoni, T. Guérin, C. Kammerer, G. Rapenne, *Chem. Eur. J.* **2019**, *25*, 16328.

11 A. Carella, G. Vives, T. Cox, J. Jaud, G. Rapenne, J.-P. Launay, *Eur. J. Inorg. Chem.,* **2006**, 980–987; G. Erbland, Y. Gisbert, G. Rapenne, C. Kammerer, *Eur. J. Org. Chem*. **2018**, 4731.

12 X. Li, Y. Gisbert, D. Sluysmans, G. Rapenne, C. Kammerer, A.-S. Duwez, *ChemRxiv* **2023**, 10.26434/chemrxiv-2023-mgq5f-v2

13 B. Martín-Matute, M. Edin, K. Bogár, F. B. Kaynak, J.-E. Bäckvall, *J. Am. Chem. Soc.,* **2005**, *127*, 8817.

Electronic Supporting Information for *Chemistry Letters*

Supplementary Information

I. Experimental section

1. Synthesis and characterisation

General methods. All chemicals and solvents were purchased from commercial suppliers and were used without further purification. 4-Dimethylaminobenzaldehyde, piperidine, potassium phosphate, tetrakis(triphenylphosphine) palladium(0), palladium(II) acetate, 2-dicyclohexylphosphino-2',6'-dimethoxybiphenyl (SPhos), cesium carbonate were purchased from Aldrich. Acetic acid was purchased from Acros.
The precursors employed in the synthesis of new target compounds **$B2_5$[Ru]**, **$B1_4B2_1$[Ru]** and **[Ru]'** were prepared according to previously reported procedures: **B1**[1], penta(*p*-bromophenyl)cyclopentadienyl hydrotris (indazolyl)borate ruthenium(II) **Br_5[Ru]**,[2] 1-(*p*-iodophenyl)-2,3,4,5-tetra(*p*-bromophenyl)cyclopentadienylhydrotris (inda-zolyl)borate ruthenium(II) **Br_4I_1[Ru]**,[3] thallium hydrotris{6-[(ethylsulfanyl)methyl] indazol-1-yl}borate **$TlTp^{4Bo,6\text{-}CH2SEt}$** [4] and bromido dicarbonyl η^5-1,2,3,4,5-pentaphenyl cyclopentadienyl ruthenium(II).[4]

All reactions were carried out using standard Schlenk techniques under an argon atmosphere. Microwave reactions were carried out by using a CEM Discover LabMate microwave reactor. Column chromatography was carried out on 230–400 mesh silica gel (Aldrich) unless otherwise stated. Thin layer chromatography (TLC) was performed on pre-coated aluminum-backed silica gel 60 UV254 plates (Macherey–Nagel) with visualization effected using ultraviolet irradiation (λ = 254, 366 nm).

^{1}H, ^{13}C, ^{11}B and ^{19}F NMR spectra were recorded on Avance 300 MHz (probe 5mm BBO BB-1H Z-GRD), Bruker Avance III HD 500 MHz (cryoprobe Prodigy 5mm BBO, 1H ATMA) and Avance 500 MHz (cryoprobe 5mm ^{1}H, ^{13}C). Residual solvent signals were used as internal references for ^{1}H and ^{13}C NMR, and ^{11}B and ^{19}F NMR spectra were referenced according to the solvent. Chemical shifts (δ) are reported in ppm. Coupling constants (*J*) are given in Hz and the following abbreviations have been used to describe the signals: singlet (s); doublet (d); triplet (t); quadruplet (q); quintuplet (quint); multiplet (m); broad (br.). Full assignments of ^{1}H and ^{13}C NMR spectra were made with the assistance of COSY, HSQC and HMBC spectra. The full width of ^{1}H NMR and ^{13}C NMR spectra is shown on purpose in the Supporting Information section; in case some minor impurities such as grease or solvent traces are present, the corresponding peaks have been assigned. It must be noted that due to the quadrupolar relaxation (proton coupled with the nuclear spin of the boron atom), the ^{1}H-NMR signal of the BH proton and the ^{11}B-NMR signal of the Boron is very broad and difficult to locate (For instance see C. Lopez et al, J. *Inorg. Chim. Acta* **1990**, *176*, 195).

High-resolution mass spectra (HRMS) were performed with a Waters Xevo G2 QTOF spectrometer for electrospray ionization (ESI). The MALDI-TOF mass spectrometry was performed using Bruker Daltonics Autoflex II spectrometer and JEOL JMS-S300 spectrometer (matrix: *trans*-2-[3-(4-*tert*-butylphenyl)-2-methyl-2-propenylidene] malononitrile DTCB). Elemental analysis was performed using a PerkinElmer 2400 Series II CHNS Organic Elemental Analyzer.

Absorption spectra were collected with a Perkin-Elmer Lambda 950 spectrophotometer by using 1 cm optical path quartz cuvettes. Spectrofluorimetric grade CH_2Cl_2 (Merck Uvasol®) was used as solvent.

Crystallographic data for compound **[Ru]'** were collected on a Bruker-AXS D8-Venture diffractometer equipped with a Photon III-C14 detector using Mo Kα radiation (λ=0.71073 Å). Phi- and omega-scans were used. Space group was determined on the basis of systematic absences and intensity statistics. Semi-empirical absorption

correction was employed.[19 5] The structure was solved using an intrinsic phasing method (SHELXT),[20 6] and refined using the least-squares method on *F2*.[21 7] All non-H atoms were refined with anisotropic displacement parameters. Hydrogen atoms were refined isotropically at calculated positions using a riding model with their isotropic displacement parameters constrained to be equal to 1.5 times the equivalent isotropic displacement parameters of their pivot atoms for terminal sp3 carbon and 1.2 times for all other carbon atoms. The solvent molecule (CH_2Cl_2) and a thioether group were found to be disordered over two positions, for which occupancies were refined. Several restraints (SAME, SIMU, DELU) were applied to refine these disordered parts and to avoid the collapse of the structure during the least-squares refinement by the large anisotropic displacement parameters. Hydrogen on boron atom was located by difference Fourier map and was freely refined.

2. Model compound B2. 4-Dimethylaminobenzaldehyde (292 mg, 1.96 mmol, 3 equiv.), piperidine (0.97 mL, 9.78 mmol, 15 equiv.) and acetic acid (19 µL, 0.33 mmol, 0.5 equiv.) were added to a solution of precursor **B1** (330 mg, 0.65 mmol, 1 equiv.) in toluene (30 mL) under argon. The resulting mixture was refluxed for 24h using a Dean–Stark apparatus. After cooling down to room temperature, the solution was extracted with dichloromethane (3 x 30 mL) and the organic layers combined. The organic phase was washed with a saturated NaCl solution (1 x 50 mL) and water (2 x 50 mL), then dried over Na_2SO_4 and the solvent was evaporated under vacuum. The crude mixture was dissolved in dichloromethane and filtered through a silica pad. The pad was rinsed with dichloromethane and methanol, and the filtrate was evaporated. The crude mixture was then purified by silica gel chromatography (SiO_2, CH_2Cl_2/MeOH gradient from 98:2 to 80:20). The pure compound **B2** was obtained in 20% yield (100 mg, 0.13 mmol) as a black powder with iridescent reflections.
R_f = 0.6 (SiO_2, pure CH_2Cl_2). **^{1}H NMR** (500 MHz, CD_2Cl_2, 25 °C): δ = 7.88 (AA'BB' pattern, 2H, H_a), 7.57 (d, ^3J=16.6 Hz, 2H, H_k), 7.53 (d, ^3J=8.5 Hz, 4H, H_h), 7.36 (AA'BB' pattern, 2H, H_b), 7.22 (d, ^3J=16.9 Hz, 2H, H_j), 6.75 (d, ^3J=8.9 Hz, 4H, H_i), 3.03 (br. s, 12H, H_d), 2.65-2.61 (m, 4H, H_e), 1.38 (s, 12H, H_c), 1.33 (s, 6H, H_g), 1.16 (t, ^3J=7.5 Hz, 6H, H_f) ppm. **^{13}C{^{1}H} NMR** (126 MHz, CD_2Cl_2, 25 °C): δ = 151.4 (C_{10}), 150.6 (C_8), 139.6 (C_3 and C_4), 138.8 (C_6), 136.5 (C_j), 135.5 (C_a), 133.9 (C_5 and C_7), 129.2 (C_2), 129.0 (C_h), 128.8 (C_b), 125.9 (C_9), 115.7 (C_k), 112.5 (C_i), 84.5 (C_1), 40.5 (C_d), 25.2 (C_c), 18.8 (C_e), 14.2 (C_f), 11.8 (C_g) ppm. **^{11}B NMR** (160 MHz, CD_2Cl_2, 25 °C): δ = 1.29 (t, J(^{11}B-^{19}F)=35.0 Hz) ppm. The signal corresponding to the boronic acid pinacol ester function could not be precisely assigned. **^{19}F NMR** (471 MHz, CD_2Cl_2, 25 °C): δ = -139.1 (q, J(^{11}B-^{19}F)=35.0 Hz) ppm. **UV-Vis** (CH_2Cl_2): λ_{max}, nm (ε_{max}, M^{-1} cm^{-1}) = 337 (35000), 419 (32000), 501 (17000), 709 (58000). **HRMS** (ESI$^+$): calcd. for $C_{47}H_{57}B_2F_2N_4O_2$ $[M+H]^+$: 769.4636, found 769.4639.

3. Model complex [Ru]'. In a 10 mL microwave reactor were placed a magnetic stir bar, bromido dicarbonyl η^5-1,2,3,4,5-pentaphenylcyclopentadienyl ruthenium(II)[18] (110 mg, 0.16 mmol, 1.0 eq.), thallium hydrotris(indazolyl)borate **TlTp$^{4Bo,6\text{-}CH2Set}$** (170 mg, 0.22 mmol, 1.35 eq.) and anhydrous acetonitrile (5 mL). The mixture was then degassed by bubbling argon for 15 minutes, before heating using microwave irradiation (115 °C, pressure up to 5 bar, 250 W, 3 x 10 minutes, releasing the pressure and manually shaking between each cycle). The resulting suspension was filtered over silica (eluted with CH_2Cl_2) and the solvents were removed *in vacuo*. The residue was purified by column chromatography (SiO_2, CH_2Cl_2/pentane 40:60 to 60:40) to give complex **[Ru]'** as an orange solid in 50% yield (91 mg, 0.08 mmol).
R_f = 0.22 (SiO_2, Hexane/CH_2Cl_2 60:40). **^{1}H NMR** (500 MHz, CD_2Cl_2, 25 °C): δ = 7.89 (br. s, 6H, H_a and H_b), 7.41 (dd, ^3J = 8.4 Hz, ^4J = 1.3 Hz, 10H, H_h), 7.28 (d, ^3J = 7.8 Hz, 3H, H_c), 7.13 (m, 5H, H_j), 7.05 - 6.99 (m, 13H, H_d and H_i), 3.90 (s, 6H, H_e), 2.47 (q, ^3J = 7.4 Hz, 6H, H_f), 1.28 (t, ^3J = 7.4 Hz, 9H, H_g) ppm. **^{13}C{^{1}H} NMR** (126 MHz, CD_2Cl_2, 25 °C): δ = 144.0 (C_3), 141.0 (C_b), 137.7 (C_2), 134.3 (C_5), 134.2 (C_h), 127.5 (C_i and C_j), 122.5 (C_4), 122.4 (C_d), 120.3 (C_c), 111.4 (C_a), 88.5 (C_1), 36.9 (C_e), 25.7 (C_f), 14.8 (C_g) ppm. **UV-Vis** (CH_2Cl_2): λ_{max},

nm (ε_{max}, M^{-1} cm^{-1}) = 268 (131000), 343 (38000). **HRMS** (ESI^+): calcd. for $C_{65}H_{60}BN_6RuS_3$ $[M+H]^+$: 1133.3201, found 1133.3201. **Elemental analysis** (%) calcd. for $C_{65}H_{59}BN_6RuS_3$: C 68.95, H 5.25, N 7.42, found: C 68.91, H 4.78, N 7.42. **Crystal data**: Crystals suitable for X-Ray diffraction analysis were obtained by slow evaporation of a 1:2 methanol/CH_2Cl_2 solution of complex **[Ru]'**. The title compound co-crystallised with dichloromethane. Selected data for **[Ru]'**: $C_{65}H_{59}BN_6RuS_3{\cdot}CH_2Cl_2$, M = 1217.16, triclinic, space group *P*$\bar{1}$, *a* = 12.1788(6) Å, *b* = 14.1325(6) Å, *c* = 18.1834(9) Å, α = 100.0807(18)°, β = 98.3306(18)°, γ = 103.7255(18)°, *V* = 2936.0(2) $Å^3$, *Z* = 2, crystal size 0.300 x 0.240 x 0.140 mm^3, 146385 reflections collected (14545 independent, R*int* = 0.0416), 783 parameters, 169 restraints, *R*1 [I>2σ(I)] = 0.0327, *wR*2 [all data] = 0.0893, largest diff. peak and hole: 1.336 and -0.864 e.$Å^{-3}$. For more details, see the Supporting Information section. CCDC-2246796 contains the supplementary crystallographic data for this paper. These data can be obtained free of charge from The Cambridge Crystallographic Data Centre.

4. Complex B2$_5$[Ru]. In a dry Schlenk tube under argon, precursor **Br$_5$[Ru]** (12 mg, 7.8 µmol, 1 equiv.), palladium(II) acetate (0.6 mg, 2.7 µmol, 0.35 equiv.), K_3PO_4 (17 mg, 78 µmol, 10 equiv.), boronic acid pinacol ester **B2** (60 mg, 78 µmol, 10 equiv.), and 2-dicyclohexylphosphino-2',6'-dimethoxybiphenyl (SPhos, 2 mg, 4.6 µmol, 0.6 equiv.) were successively introduced into degassed toluene/ethanol/water (2:2:1, 2.5 mL). The resulting suspension was stirred at 100 °C for 48 hours, and completion of the reaction was monitored by TLC (SiO_2, CH_2Cl_2/cyclohexane 1:1). The reaction mixture was cooled to room temperature, and the solvents evaporated. The crude residue was then triturated in ethyl acetate and the solid was recovered by filtration and washed several times with ethyl acetate. The brownish, iridescent powder was isolated as pure ruthenium complex **B2$_5$[Ru]** in 74% yield (25 mg, 5.8 µmol).
***R*$_f$** = 0.9 (SiO_2, CH_2Cl_2/MeOH 99.5:0.5). **^{1}H NMR** (500 MHz, CD_2Cl_2, 25 °C): δ = 8.13 (s, 3H, H_a), 7.99 (s, 3H, H_b), 7.74 (m, 20H, H_q and H_s), 7.59-7.51 (m, 40H, H_k and H_m and H_r), 7.44 (d, ^3J=8.6 Hz, 3H, H_c), 7.37 (d, ^3J=7.9 Hz, 10H, H_p), 7.22 (d, ^3J=16.4 Hz, 10H, H_l), 7.09 (d, ^3J=8.6 Hz, 3H, H_d), 6.73 (d, ^3J=8.4 Hz, 20H, H_n), 3.95 (s, 6H, H_e), 3.01 (s, 60H, H_o), 2.62 (br q, ^3J=8.1 Hz, 20H, H_i), 2.51 (q, ^3J=7.4 Hz, 6H, H_f), 1.37 (s, 30H, H_h), 1.30 (t, ^3J=7.4 Hz, 9H, H_g), 1.15 (t, ^3J=7.5 Hz, 30H, H_j) ppm. **^{13}C{^{1}H} NMR** (126 MHz, CD_2Cl_2, 25 °C): δ = 151.4 (C_{12}), 150.6 (C_{10}), 144.2 (C_{13}), 141.2 (C_a), 140.8 (C_4), 139.2 (C_3 and C_6), 138.7 (C_8), 138.1 (C_{15}), 136.5 (C_l), 135.9 (C_5), 135.0 (C_s), 133.9 (C_2 and C_7 and C_9), 130.0 (C_p), 129.0 (C_m), 127.6 (C_q), 126.1 (C_r), 125.9 (C_{11}), 122.7 (C_d), 122.6 (C_{14}), 120.5 (C_c), 115.7 (C_k), 112.5 (C_n), 111.5 (C_b), 88.6 (C_1), 40.5 (C_o), 37.0 (C_e), 25.8 (C_f), 18.8 (C_i), 14.8 (C_g), 14.3 (C_j), 11.9 (C_h) ppm. **^{11}B NMR** (160 MHz, CD_2Cl_2, 25 °C): δ = 1.32 (t, J(^{11}B-^{19}F)=35.0 Hz) ppm. **^{19}F NMR** (471 MHz, CD_2Cl_2, 25 °C): δ = -139.1 (m) ppm. **UV-Vis** (CH_2Cl_2): λ_{max}, nm (ε_{max}, M^{-1} cm^{-1}) = 273 (116000), 335 (189000), 420 (154000), 503 (88000), 711 (248000). **HRMS** (MALDI): calcd. for $C_{270}H_{274}B_6F_{10}N_{26}RuS_3$ $[M]^+$: 4335.0970, found 4335.1084.

5. Complex Br$_4$B2$_1$[Ru]. In a dry Schlenk tube under argon, precursor **Br$_4$I$_1$[Ru]** (60 mg, 38 µmol, 1 equiv.), $Pd(PPh_3)_4$ (4.4 mg, 3.8 µmol, 0.1 equiv.), cesium carbonate (25 mg, 76 µmol, 2 equiv.) and boronic acid pinacol ester **B2** (30 mg, 38 µmol, 1 equiv.) were successively introduced into a mixture of degassed THF/DMF/water (2:4:0.5, 6.5 mL). The resulting mixture was stirred at 70 °C for 20 hours, and completion of the reaction was monitored by TLC (SiO_2, CH_2Cl_2/cyclohexane 75:25). Upon completion of the reaction, the crude mixture was allowed to cool to room temperature and evaporated to dryness. The crude solid was dissolved in 50 mL of dichloromethane and washed with 2 x 10mL of water. The organic phase was then dried over $MgSO_4$ and evaporated. The crude compound was purified by flash chromatography on basic alumina, using mixtures of dichloromethane and cyclohexane as eluent, to afford the pure compound **Br$_4$B2$_1$[Ru]** as a black solid with red-brown reflections in 63% yield (50 mg, 24 µmol).
***R*$_f$** = 0.65 (SiO_2, CH_2Cl_2/cyclohexane 75:25). **^{1}H NMR** (500 MHz, CD_2Cl_2, 25 °C): δ = 7.90 (s, 3H, H_a), 7.87 (s, 3H, H_b), 7.71 (d, ^3J=8.1 Hz, 2H, H_r), 7.58-7.51 (m, 6H, H_l and H_m), 7.46 (s, 4H, H_p and H_q), 7.37-7.35 (m, 5H, H_c and H_s), 7.34-7.31 (m, 4H, H_{19} or $H_{19'}$), 7.28-7.25 (m,

4H, H_{19} or $H_{19'}$), 7.23-7.19 (m, 10H, H_k and H_{20} and $H_{20'}$), 7.05 (dd, ^3J=8.4 Hz, ^4J=1.4 Hz, 3H, H_d), 6.75 (d, ^3J=8.5 Hz, 4H, H_n), 3.91 (s, 6H, H_e), 3.03 (s, 12H, H_o), 2.65-2.60 (m, 4H, H_i), 2.47 (q, ^3J=7.4 Hz, 6H, H_f), 1.37 (s, 6H, H_h), 1.28 (t, ^3J=7.4 Hz, 9H, H_g), 1.16 (t, ^3J=7.5 Hz, 6H, H_j) ppm. **^{13}C{^{1}H} NMR** (126 MHz, CD_2Cl_2, 25 °C): δ = 151.4 (C_{14}), 150.6 (C_{12}), 144.1 (C_{15}), 140.7 (C_b), 140.6 (C_6), 139.5 (C_5), 138.7 (C_8), 138.2 (C_{17}), 136.5 (C_k), 136.4 (C_{10}), 136.0 (C_7), 135.7 (C_{19} or $C_{19'}$), 135.6 (C_{19} or $C_{19'}$), 134.5 (C_p), 133.9 (C_{11}), 133.1 (C_4), 133.0 ($C_{18'}$), 132.8 (C_9), 132.7 (C_{18}), 131.1 (C_{20} and $C_{20'}$), 130.0 (C_s), 129.0 (C_m), 127.6 (C_r), 126.2 (C_q), 125.9 (C_{13}), 122.7 (C_d), 122.5 (C_{16}), 122.3 (C_{21} or $C_{21'}$), 122.2 (C_{21} or $C_{21'}$), 120.4 (C_c), 115.7 (C_l), 112.5 (C_n), 111.4 (C_a), 88.8 (C_1), 87.7 (C_2 or C_3), 87.1 (C_2 or C_3), 40.5 (C_o), 36.9 (C_e), 25.7 (C_f), 18.8 (C_i), 14.8 (C_g), 14.2 (C_j), 11.9 (C_h) ppm. **^{11}B NMR** (160 MHz, CD_2Cl_2, 25 °C): δ = 1.30 (t, J(^{11}B-^{19}F)=34.7 Hz) ppm. **^{19}F NMR** (471 MHz, CD_2Cl_2, 25 °C): δ = -139.2 (q, J(^{11}B-^{19}F)=35.0 Hz) ppm. **HRMS** (MALDI): calcd. for $C_{106}H_{98}B_2Br_4F_2N_{10}RuS_3$ $[M]^+$: 2088.3079, found 2088.3196.

6. Complex B1$_4$B2$_1$[Ru]. In a dry Schlenk tube under argon, ruthenium complex **Br$_4$B2$_1$[Ru]** (40 mg, 19 µmol, 1 equiv.), palladium(II) acetate (1.5 mg, 6.7 µmol, 0.35 equiv.), K_3PO_4 (41 mg, 190 µmol, 10 equiv.), boronic acid pinacol ester **B1** (78 mg, 150 µmmol, 8 equiv.) and 2-dicyclohexylphosphino-2',6'-dimethoxybiphenyl (SPhos, 4.7 mg, 11 µmol, 0.6 equiv.) were successively introduced into a mixture of degassed toluene/ethanol/water (4:2:1, 7 mL). The resulting suspension was stirred at 110 °C for 48 hours, and completion of the reaction was monitored by TLC (SiO_2, pure CH_2Cl_2). Upon completion of the reaction, the crude mixture was allowed to cool to room temperature, evaporated to dryness and dichloromethane was added. The organic phase was washed with water (2 x 30 mL), dried over $MgSO_4$ and evaporated. Column chromatography was carried out on basic alumina (activity I) eluting with a gradient of CH_2Cl_2/cyclohexane from 30:70 to 100:0 and the pure compound **B1$_4$B2$_1$[Ru]** was isolated in 32% yield (20 mg, 6.1 µmol) as a dark pink solid with green reflections.
***R*$_f$** = 0.5 (SiO_2, CH_2Cl_2/MeOH 99.5:0.5). **^{1}H NMR** (500 MHz, CD_2Cl_2, 25 °C): δ = 8.09 (s, 3H, H_a), 7.97 (s, 3H, H_b), 7.74-7.71 (m, 20H, H_q and $H_{q'}$ and H_s and $H_{s'}$), 7.57-7.51 (m, 16H, $H_{k'}$ and H_m and H_r and $H_{r'}$), 7.40 (d, ^3J=8.4 Hz, 3H, H_c), 7.36 (d, ^3J=8.0 Hz, 2H, $H_{p'}$), 7.32 (dd, ^3J=8.4 Hz, ^4J=2.2 Hz, 8H, H_p), 7.22 (br. d, ^3J=15.1 Hz, 2H, H_l), 7.06 (dd, ^3J=8.4 Hz, ^4J=1.4 Hz, 3H, H_d), 6.74 (d, ^3J=8.4 Hz, 4H, H_n), 3.94 (s, 6H, H_e), 3.03 (br. s, 12H, H_o), 2.61 (m, 4H, $H_{i'}$), 2.50 (q, ^3J=7.4 Hz, 6H, H_f), 2.47 (s, 24H, H_k), 2.30 (q, ^3J=7.4 Hz, 16H, H_i), 1.35 (s, 6H, $H_{h'}$), 1.32 (s, 24H, H_h), 1.30 (t, ^3J=7.4 Hz, 9H, H_g), 1.14 (t, ^3J=7.5 Hz, 6H, $H_{j'}$), 0.96 (t, ^3J=7.4 Hz, 24H, H_j) ppm. **^{13}C{^{1}H} NMR** (126 MHz, CD_2Cl_2, 25 °C): δ = 154.1 (C_{10}), 151.4 (C_{12}), 144.2 (C_{13}), 141.1 (C_a), 140.8 (C_4 and $C_{4'}$), 140.7 ($C_{10'}$), 140.4 (C_6), 139.2 ($C_{8'}$), 139.2 (C_3 and $C_{3'}$), 139.2 ($C_{6'}$), 138.9 (C_8), 138.0 (C_{15}), 136.4 (C_l), 135.3 (C_5 and $C_{5'}$), 135.0 (C_s and $C_{s'}$), 133. 9 (C_2 and $C_{2'}$), 133.8 ($C_{7'}$ and $C_{9'}$), 133.3 (C_9), 131.3 ($C_{p'}$), 131.0 (C_7), 129.3 (C_p), 129.0 (C_m), 127.6 (C_q), 127.5 ($C_{q'}$), 126.1 (C_r and $C_{r'}$), 125.9 (C_{11}), 122.6 (C_d), 122.6 (C_{14}), 120.4 (C_c), 115.6 ($C_{k'}$), 112.5 (C_n), 111.5 (C_b), 88.6 ($C_{1'}$), 88.5 (C_1 and $C_{1''}$), 40.5 (C_o), 37.0 (C_e), 25.8 (C_f), 19.1 ($C_{i'}$), 17.4 (C_i), 14.8 (C_g and C_j), 14.3 ($C_{j'}$), 12.7 (C_k), 12.2 (C_h), 11.9 ($C_{h'}$) ppm. C_l did not appear on the ^{13}C{^{1}H} spectrum but its chemical shift was assigned thanks to correlations on HSQC and HMBC NMR spectra. **^{11}B NMR** (160 MHz, CD_2Cl_2, 25 °C): δ = 1.29 (t, J(^{11}B-^{19}F)=32.7 Hz), 0.74 (t, J(^{11}B-^{19}F)=33.6 Hz) ppm. **^{19}F NMR** (471 MHz, CD_2Cl_2, 25 °C): δ = -139.3 (m, 2F), -145.7 (m, 8F) ppm. **UV-Vis** (CH_2Cl_2): λ_{max}, nm (ε_{max}, M^{-1} cm^{-1}) = 271 (108000), 339 (72000), 403 (42000), 526 (194000), 711 (44000). **HRMS** (MALDI): calcd. for $C_{198}H_{203}B_6F_{10}N_{18}RuS_3$ $[M+H]^+$: 3286.5076, found 3286.5120.

7.References

1. G. Erbland, S. Abid, Y. Gisbert, N. Saffon-Merceron, Y. Hashimoto, L. Andreoni, T. Guérin, C. Kammerer and G. Rapenne, *Chem. Eur. J.*, **2019**, *25*, 16328.
2. G. Erbland, Y. Gisbert, G. Rapenne and C. Kammerer, *Eur. J. Org. Chem*., **2018**, 4731.
3. Y. Gisbert, S. Abid, G. Bertrand, N. Saffon-Merceron, C. Kammerer and G. Rapenne, *Chem. Commun.,* **2019**, *55*, 14689.

4. B. Martín-Matute, M. Edin, K. Bogár, F. B. Kaynak and J.-E. Bäckvall, *J. Am. Chem. Soc.,* **2005**, *127*, 8817.
5. Bruker, SADABS, Bruker AXS Inc., Madison, Wisconsin, USA, **2008**.
6. ShelXT, G. M. Sheldrick, University of Göttingen, *Acta Crystallogr. Sect. A,* **2015**, *71*, 3-8.
7. ShelXL, G. M. Sheldrick, University of Göttingen, *Acta Crystallogr. Sect. C,* **2015**, *71*, 3-8.

II. NMR spectra of new compounds

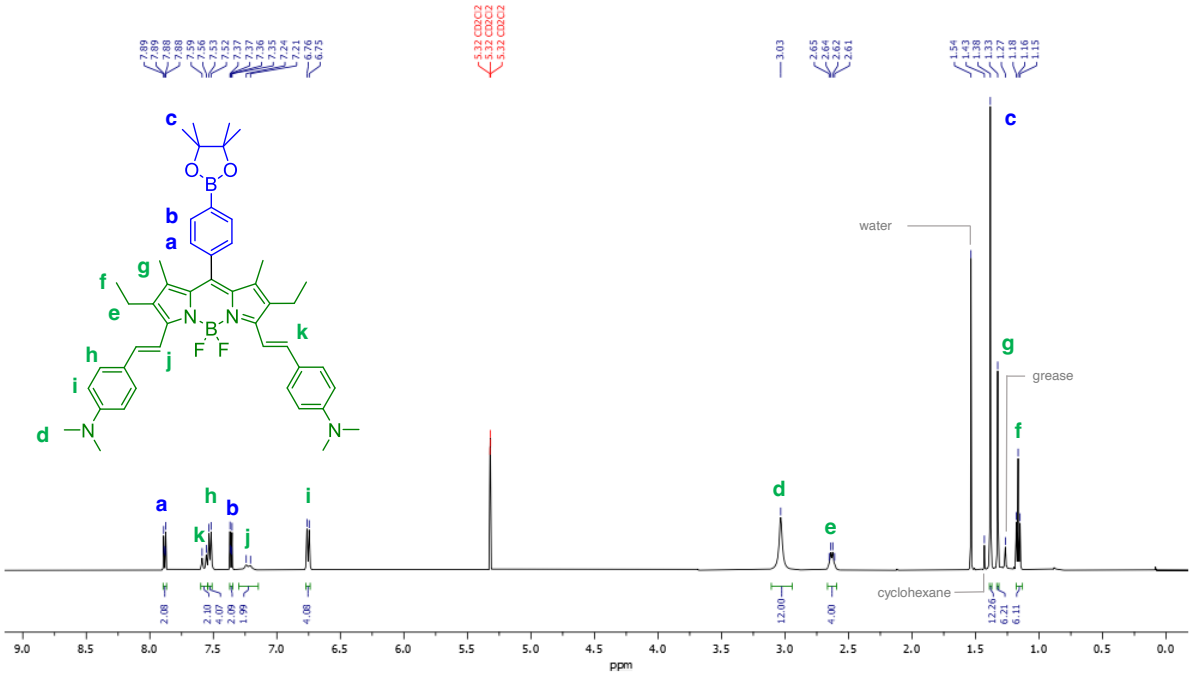

Fig. S1. ^{1}H NMR spectrum (500 MHz) of compound **B2** in CD_2Cl_2 recorded at 25 °C.

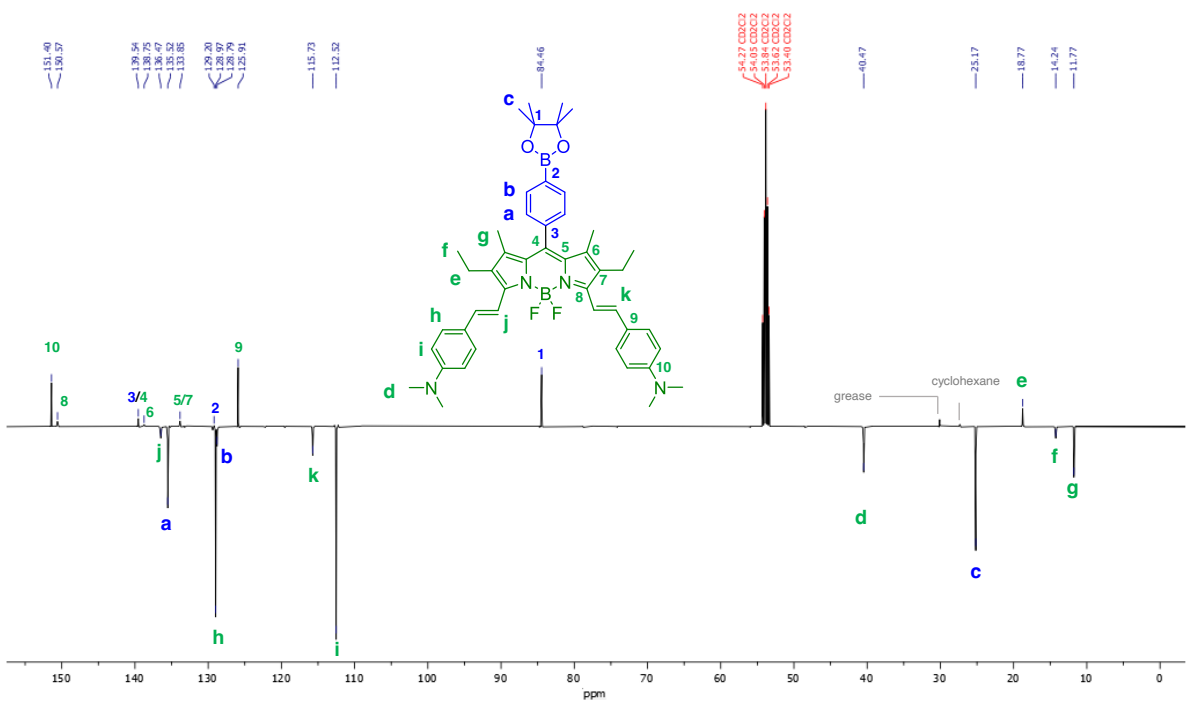

Fig. S2. ^{13}C NMR spectrum (126 MHz - JMOD) of compound **B2** in CD_2Cl_2 recorded at 25 °C.

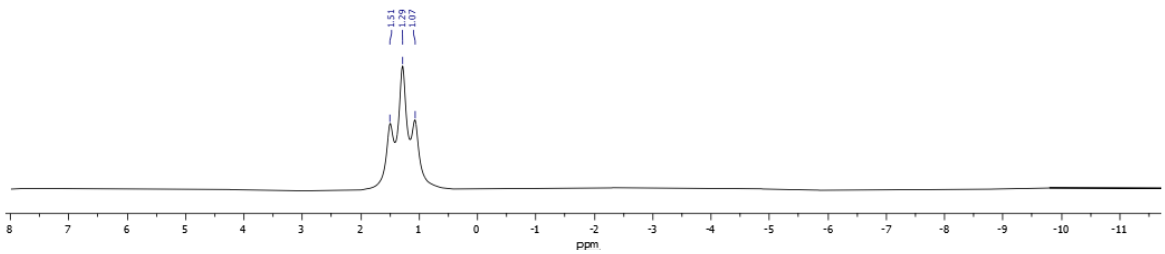

Fig. S3. ^{11}B NMR spectrum (160 MHz) of compound **B2** in CD_2Cl_2 recorded at 25 °C.

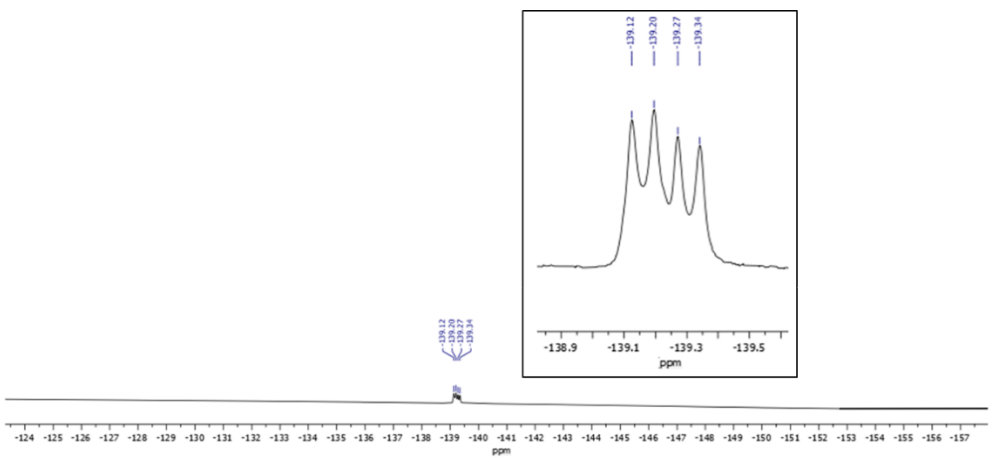

Fig. S4. ^{19}F NMR spectrum (471 MHz) of compound **B2** in CD_2Cl_2 recorded at 25 °C and zoom between -138.9 and -139.5ppm.

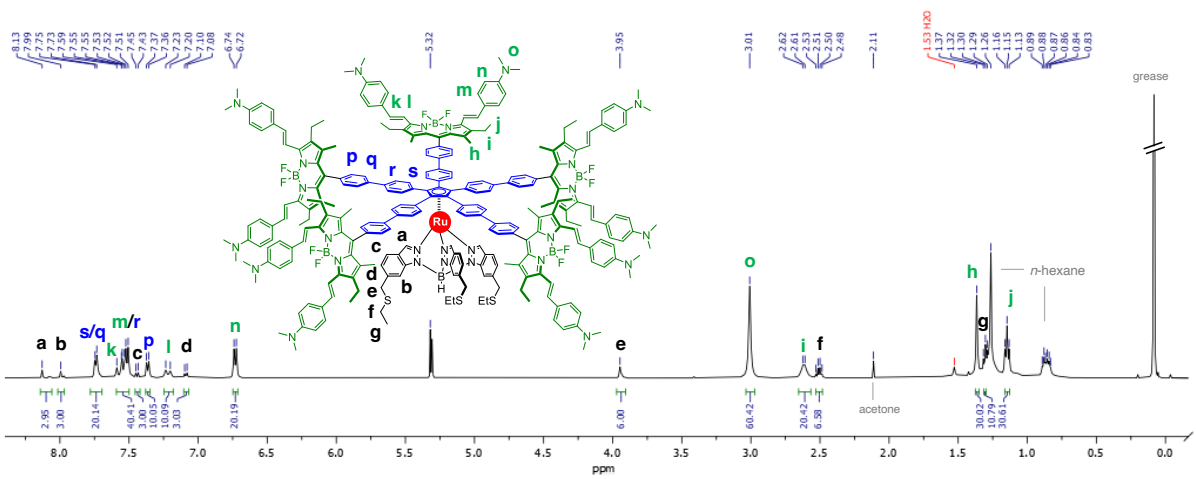

Fig. S5. ^{1}H NMR spectrum (500 MHz) of complex **B2$_5$[Ru]** in CD_2Cl_2 recorded at 25 °C.

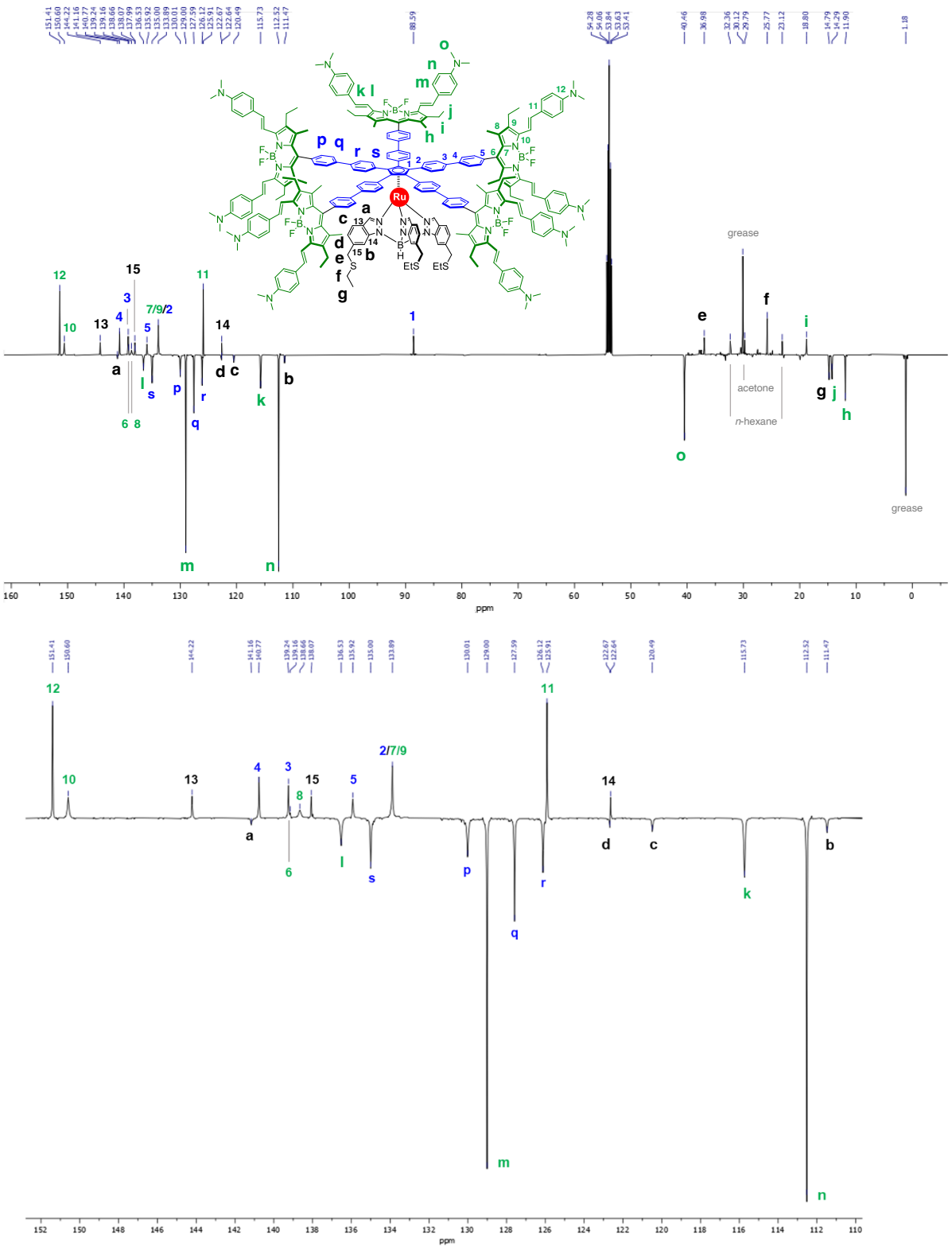

Fig. S6. ^{13}C NMR spectrum (126 MHz - JMOD) of complex **B2$_5$[Ru]** in CD_2Cl_2 recorded at 25 °C, with a zoom of the 110-152 ppm region (bottom).

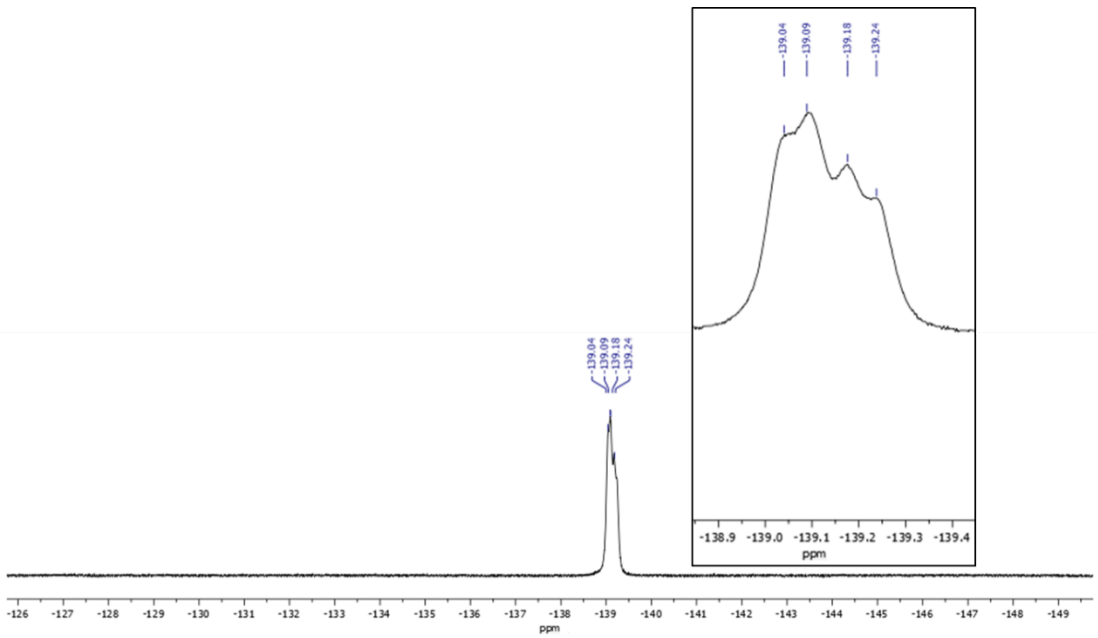

Fig. S7. ^{19}F NMR spectrum (471 MHz) of complex **B2$_5$[Ru]** in CD_2Cl_2 recorded at 25 °C and zoom between -138.9 and -139.4 ppm.

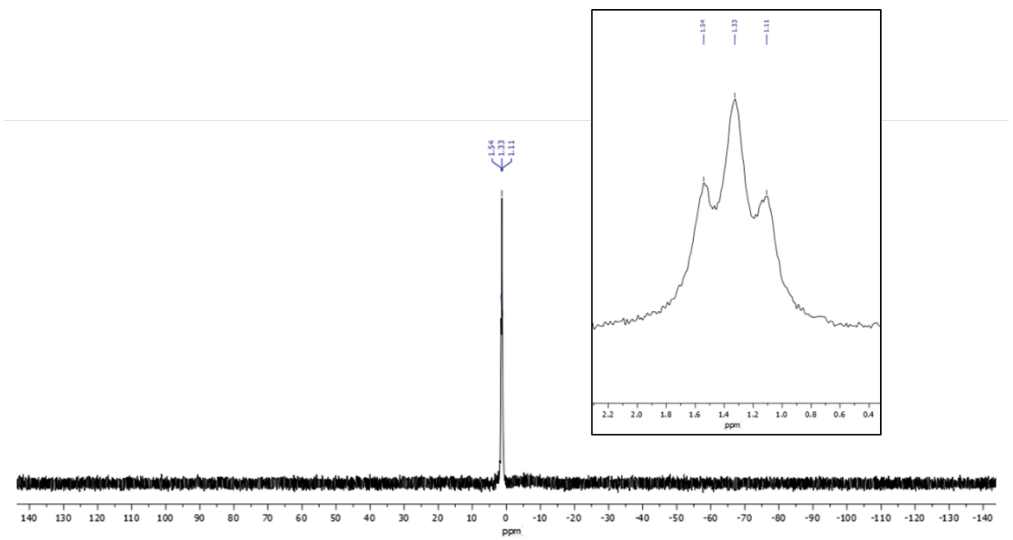

Fig. S8. ^{11}B NMR spectrum (160 MHz) of complex **B2$_5$[Ru]** in CD_2Cl_2 recorded at 25 °C, and zoom between 2.2 and 0.4 ppm.

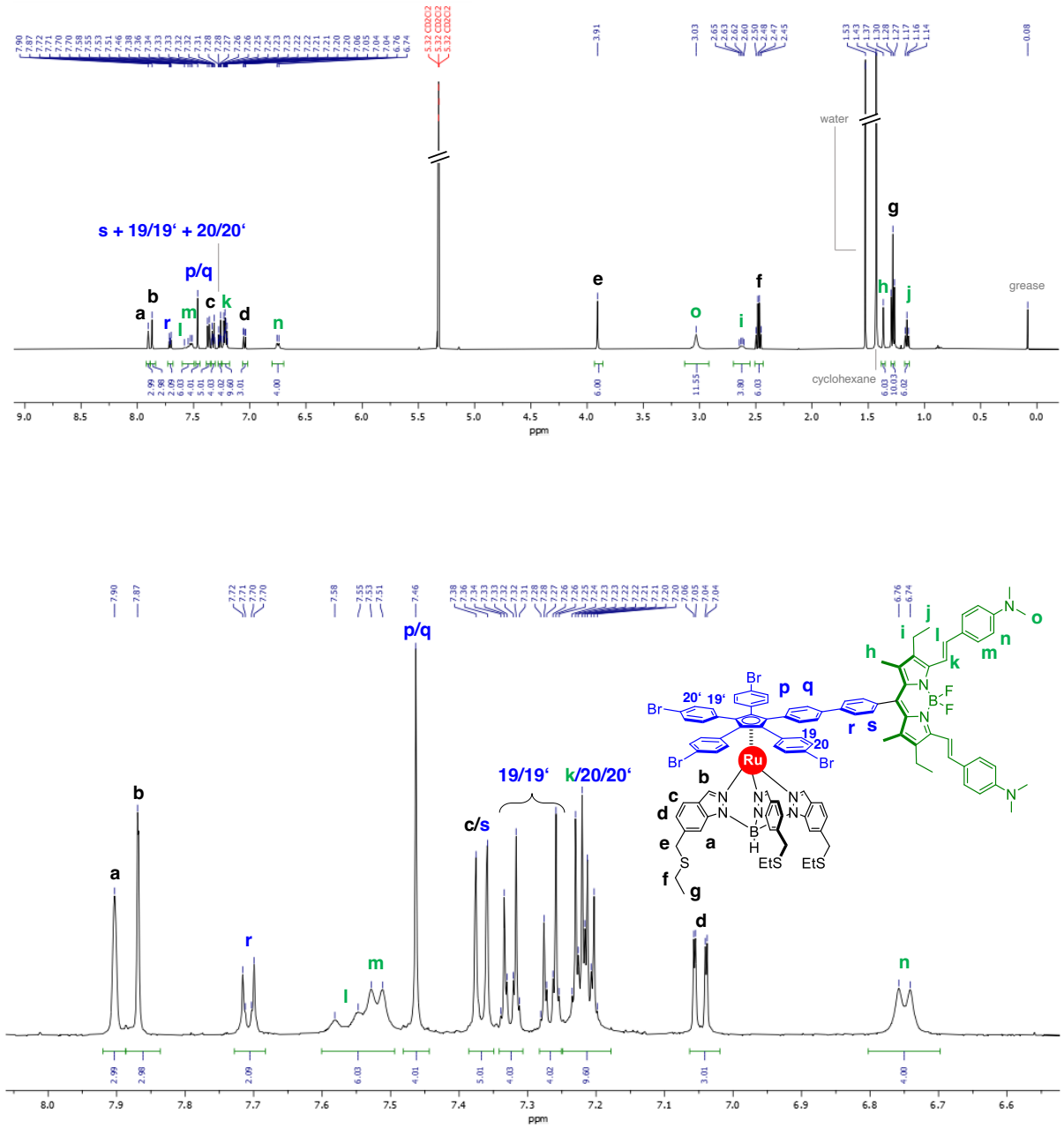

Fig. S9. ^{1}H NMR spectrum (500 MHz) of complex **Br$_4$B2[Ru]** in CD_2Cl_2 recorded at 25 °C and zoom of the 8.0-6.6 ppm region(bottom).

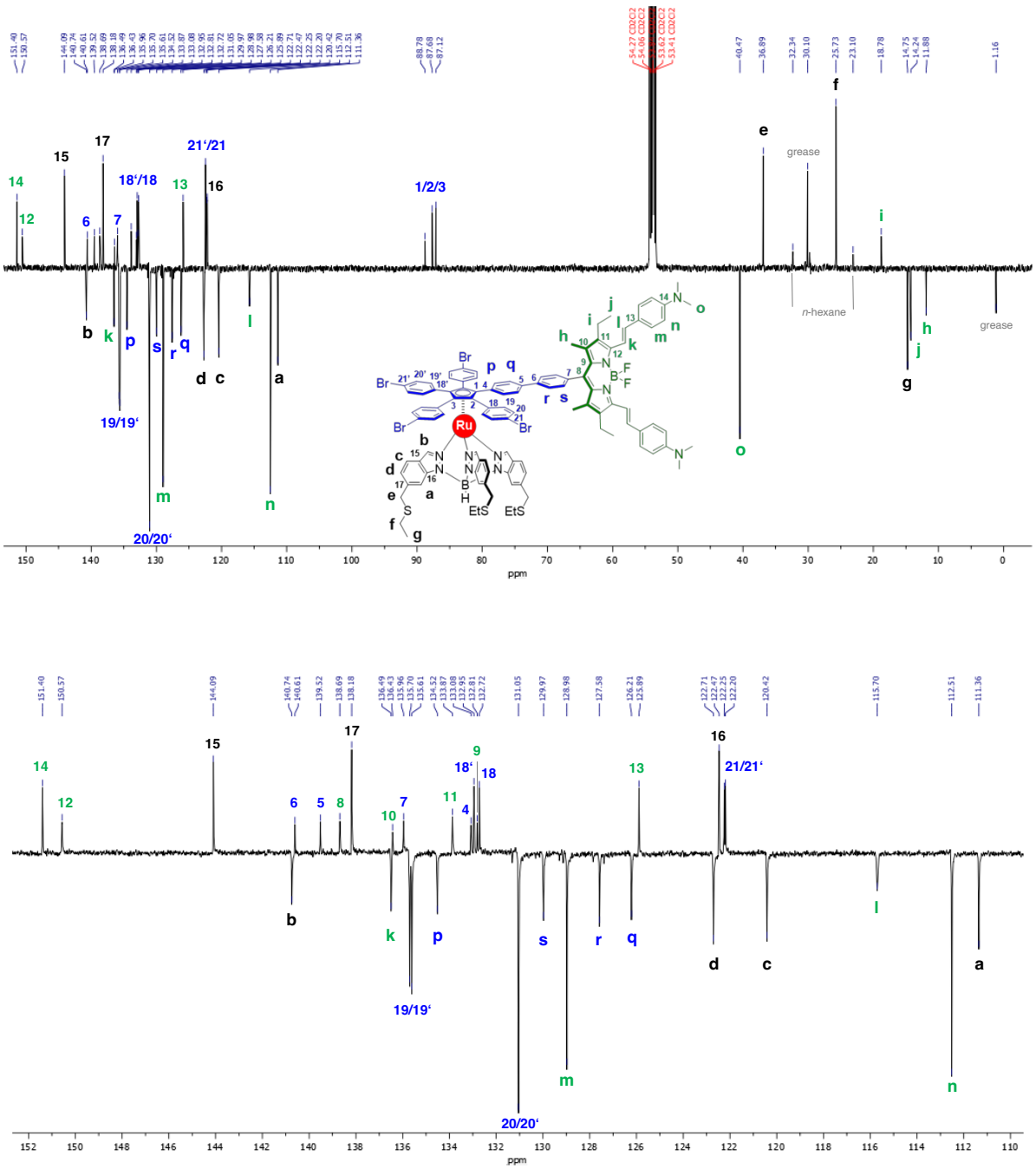

Fig. S10. ^{13}C NMR spectrum (126 MHz - JMOD) of complex **Br$_4$B2[Ru]** in CD_2Cl_2 recorded at 25 °C and zoom of the 152-110 ppm region (bottom).

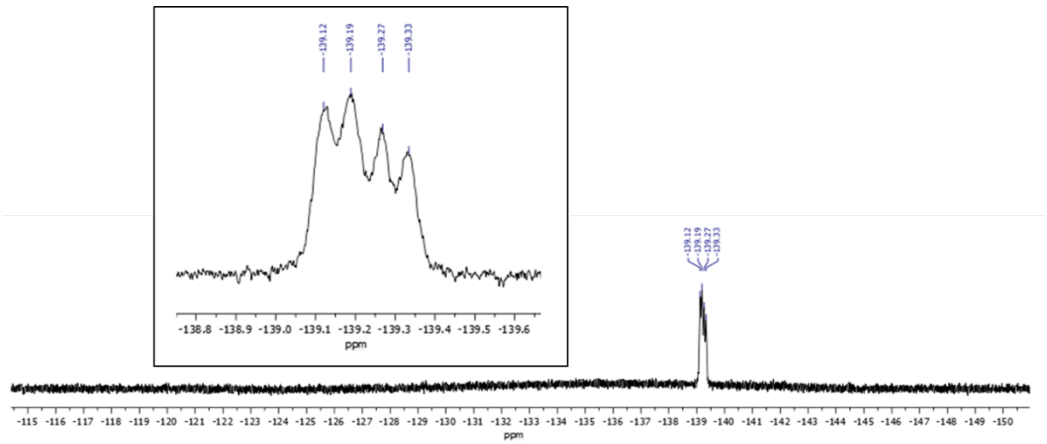

Fig. S11. ^{19}F NMR spectrum (471 MHz) of complex **Br_4B2[Ru]** in CD_2Cl_2 recorded at 25 °C and zoom between -138.8 and -139.6 ppm.

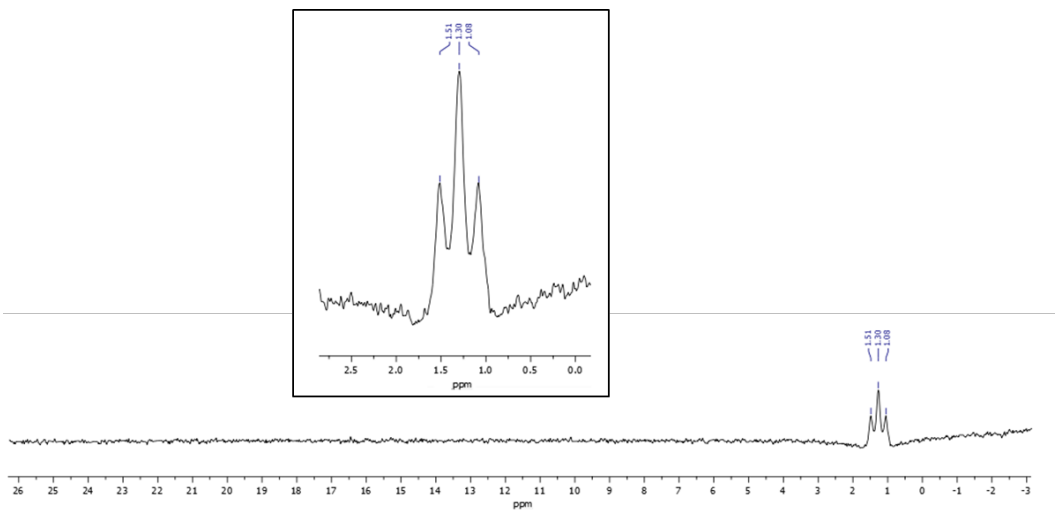

Fig. S12. ^{11}B NMR spectrum (160 MHz) of complex **Br_4B2[Ru]** in CD_2Cl_2 recorded at 25 °C and zoom between 2.5 and 0.0 ppm.

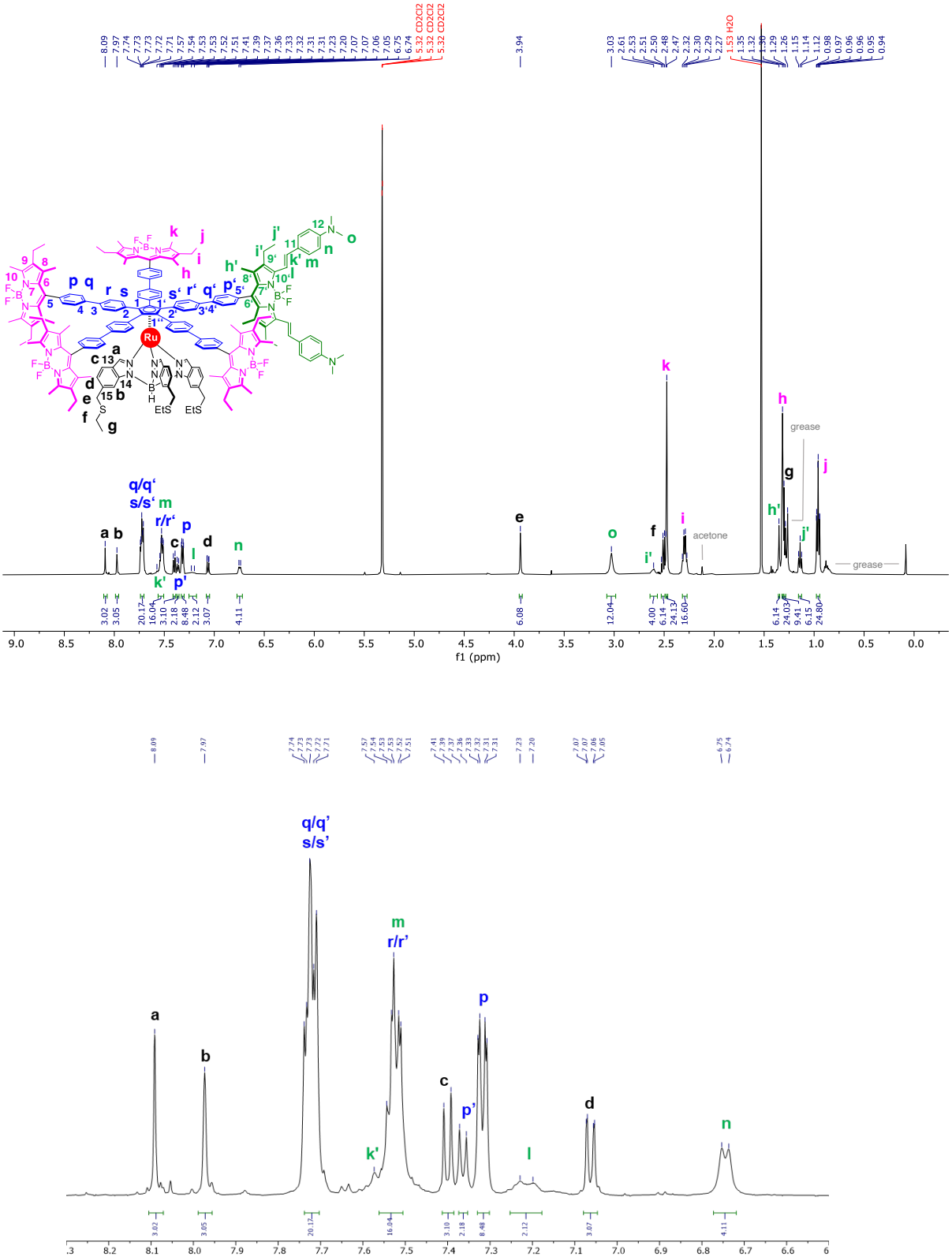

Fig. S13. ^{1}H NMR spectrum (500 MHz) of complex **$B1_4B2_1$[Ru]** in CD_2Cl_2 recorded at 25 °C and zoom of the 6.5-8.3 ppm region.

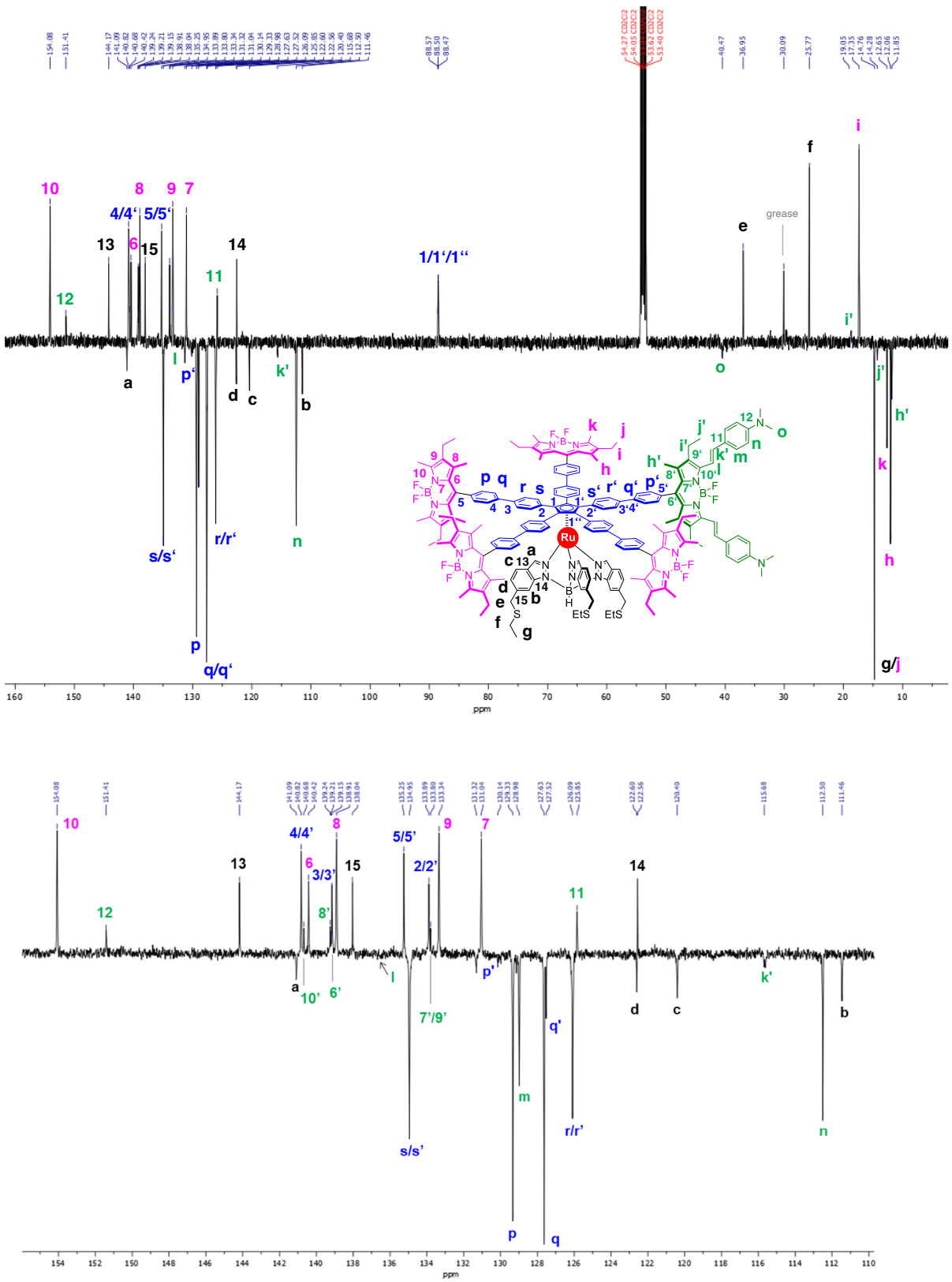

Fig. S14. ^{13}C NMR spectrum (126 MHz - JMOD) of complex **B1$_4$B2$_1$[Ru]** in CD_2Cl_2 recorded at 25 °C and zoom of the 110-154 ppm region (bottom).

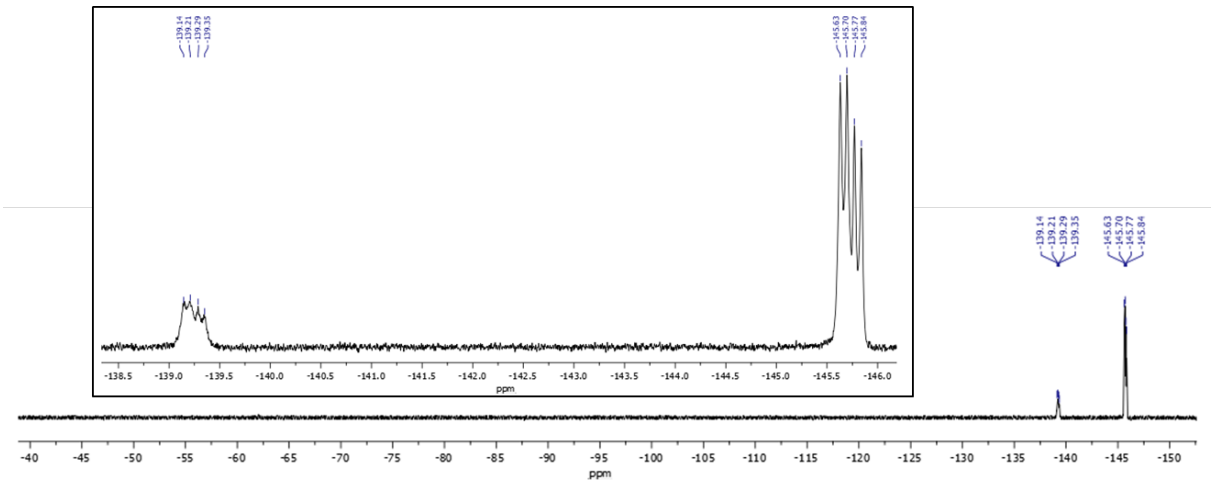

Fig. S15. ^{19}F NMR spectrum (471 MHz) of complex **$B1_4B2_1$[Ru]** in CD_2Cl_2 recorded at 25 °C and zoom between -138.5 and -146.0ppm

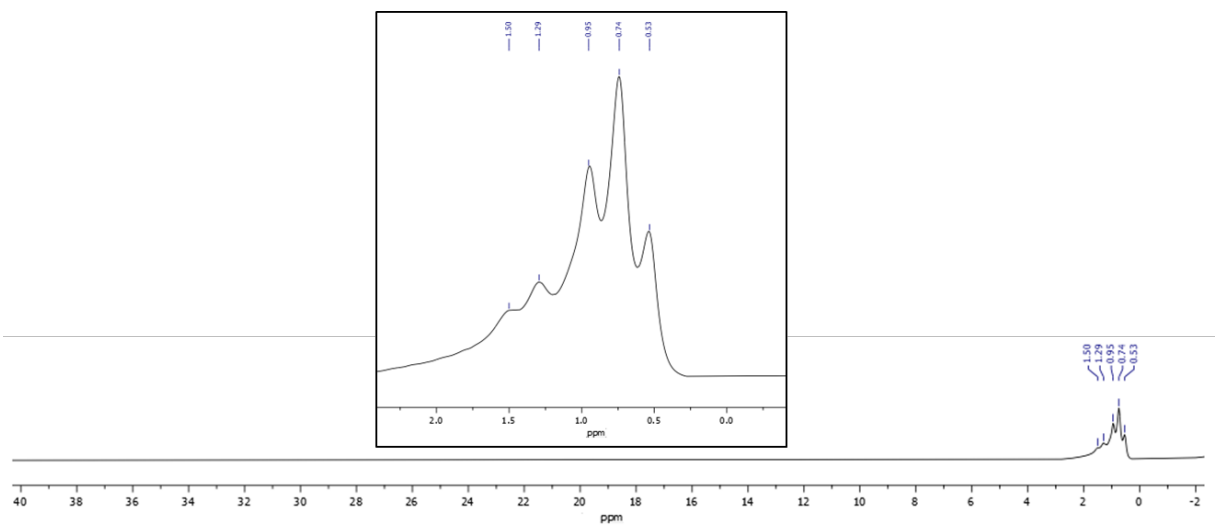

Fig. S16. ^{11}B NMR spectrum (160 MHz) of complex **$B1_4B2_1$[Ru]** in CD_2Cl_2 recorded at 25 °C and zoom between 2.0 and 0.0 ppm

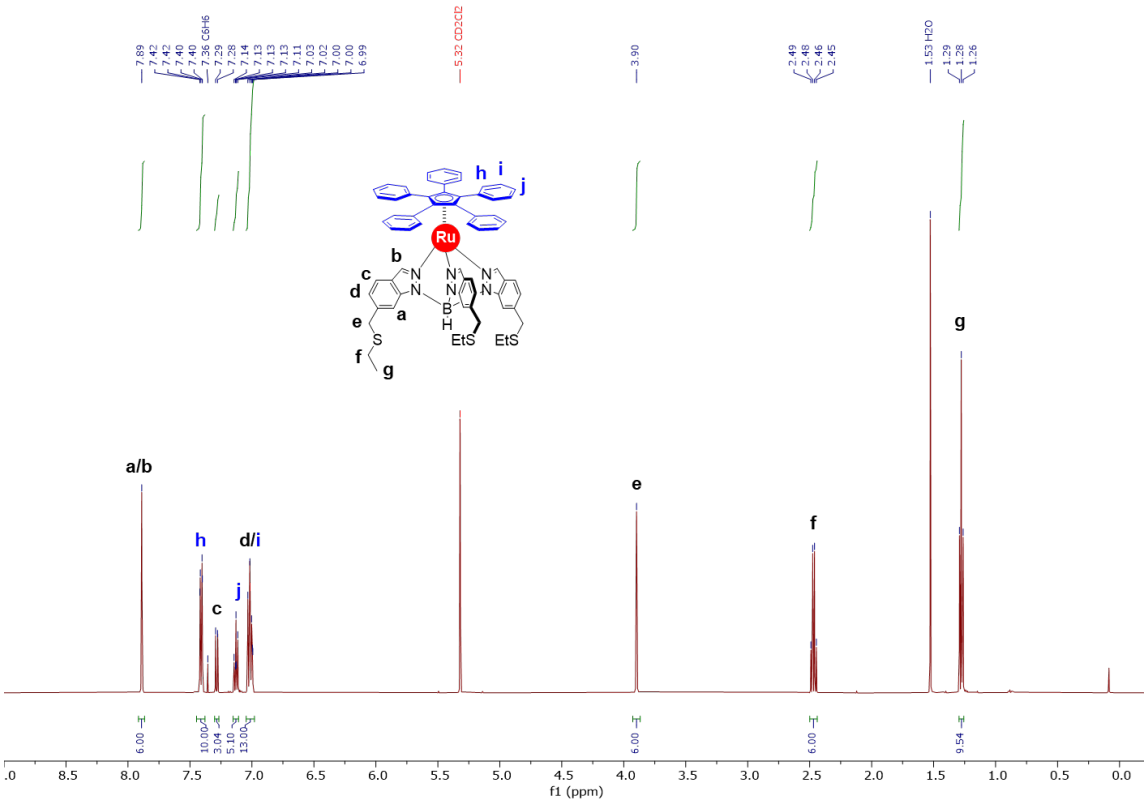

Fig. S17. ^{1}H NMR spectrum (500 MHz) of complex **[Ru]'** in CD_2Cl_2 recorded at 25 °C.

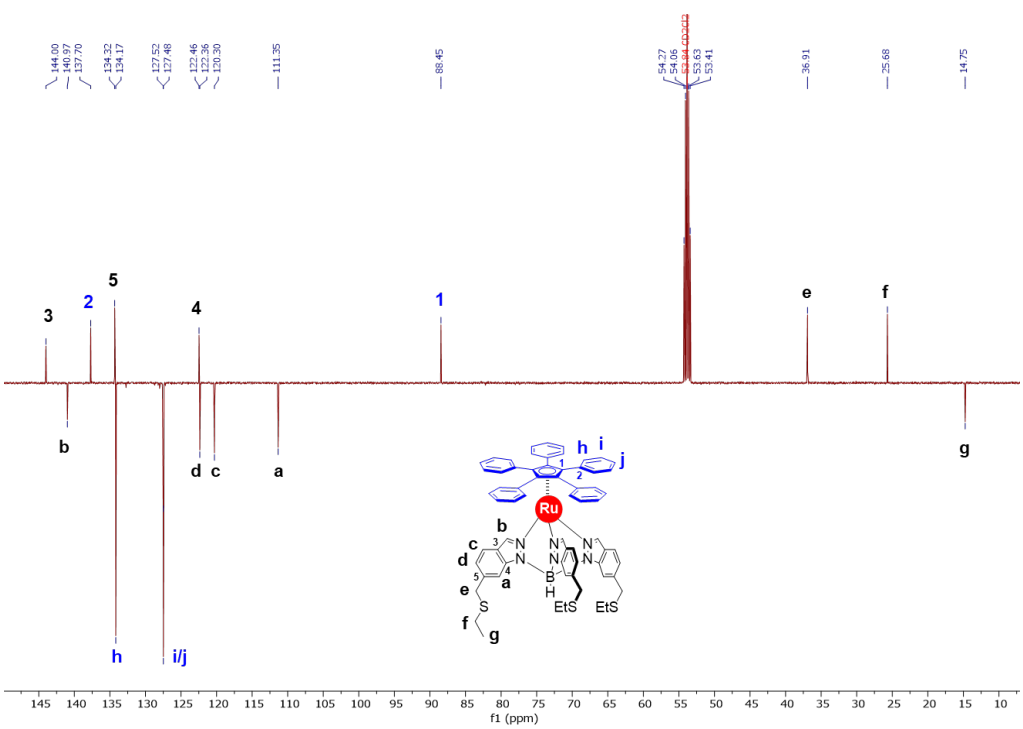

Fig. S18. ^{13}C NMR spectrum (126 MHz - JMOD) of complex **[Ru]'** in CD_2Cl_2 recorded at 25 °C.

IV. Crystallographic data for the model compound [Ru]'

Crystals suitable for X-Ray diffraction analysis were obtained by slow evaporation of a 1:2 methanol/CH_2Cl_2 solution of complex **[Ru]'**. The title compound co-crystallised with dichloromethane.

CCDC-2246796 contains the supplementary crystallographic data for this paper. These data can be obtained free of charge from The Cambridge Crystallographic Data Centre via https://www.ccdc.cam.ac.uk/structures.

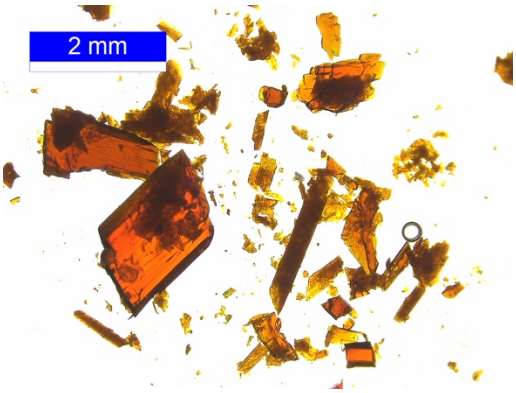

Fig. S22. Picture of the crystals of complex **[Ru]'**.

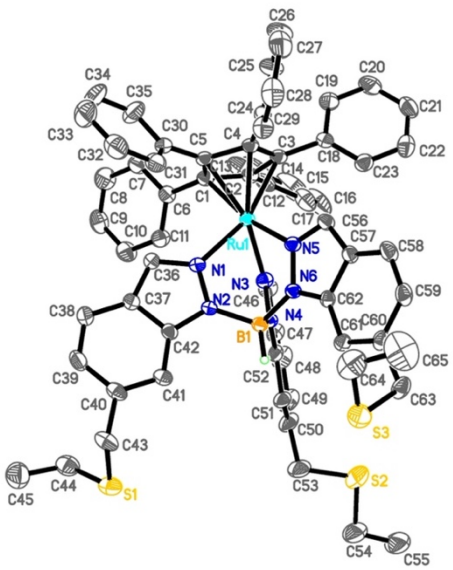

Fig. S23. Molecular structure of ruthenium complex **[Ru]'**. Thermal ellipsoids are drawn at 30% probability, and hydrogen atoms (except for B–H), solvent molecule and disordered atoms are omitted for clarity.

Table S1. Crystal data and structure refinement for complex **[Ru]'**.

Empirical formula	$C_{65}H_{59}BN_6RuS_3 \cdot CH_2Cl_2$	
Formula weight	1217.16	
Temperature	193(2) K	
Wavelength	0.71073 Å	
Crystal system	Triclinic	
Space group	$P\bar{1}$	
Unit cell dimensions	a = 12.1788(6) Å	α = 100.0807(18)°.
	b = 14.1325(6) Å	β = 98.3306(18)°.
	c = 18.1834(9) Å	γ = 103.7255(18)°.
Volume	2936.0(2) $Å^3$	
Z	2	
Density (calculated)	1.377 Mg/m^3	
Absorption coefficient	0.512 mm^{-1}	
F(000)	1260	
Crystal size	0.300 x 0.240 x 0.140 mm^3	
Theta range for data collection	3.009 to 28.297°.	
Index ranges	-16<=h<=16, -18<=k<=18, -24<=l<=24	
Reflections collected	146385	
Independent reflections	14545 [R(int) = 0.0416]	
Completeness to theta = 25.242°	99.6 %	
Absorption correction	Semi-empirical from equivalents	
Max. and min. transmission	0.7457 and 0.7008	
Refinement method	Full-matrix least-squares on F^2	
Data / restraints / parameters	14545 / 169 / 783	
Goodness-of-fit on F^2	1.047	
Final R indices [I>2sigma(I)]	R1 = 0.0327, wR2 = 0.0850	
R indices (all data)	R1 = 0.0390, wR2 = 0.0893	
Extinction coefficient	n/a	
Largest diff. peak and hole	1.336 and -0.864 e.$Å^{-3}$	